https://doi.org/10.26599/FRICT.2026.9441272

Review Article

Mechanical friction-reduction strategies in triboelectric nanogenerators for enhancing efficiency and durability: A comprehensive review

Jie Cao[ab#], Zhelin Jin[a#], Ruifei Luan[bc], Likun Gong[bc], Guoxu Liu[bc], Zhichao Jiang[bd], Jianhua Zeng[e], Guizhang Ju[a], Letian Mi[a], Guanggui Cheng[a*], Chi Zhang[bc*], Jianning Ding[a*]

[a] School of Mechanical Engineering, Jiangsu University, Zhenjiang 212013, China

[b] CAS Center for Excellence in Nanoscience, Beijing Key Laboratory of Micro-nano Energy and Sensor, Beijing Institute of Nanoenergy and Nanosystems, Chinese Academy of Sciences, Beijing 101400, China

[c] School of Nanoscience and Technology, University of Chinese Academy of Sciences, Beijing 100049, China

[d] School of Physical Science & Technology, Guangxi University, Nanning 530004, China

[e] School of Mechanical and Electrical Engineering, Guilin University of Electronic Technology, Guilin 541004, China

[#] Jie Cao and Zhelin Jin contributed equally to this work.

* Guanggui Cheng: ggcheng@ujs.edu.cn

Chi Zhang: czhang@binn.cas.cn

Jianning Ding: dingjn@ujs.edu.cn

Received: February 12, 2026; Revised: April 17, 2026; Accepted: May 22, 2026

Abstract

Triboelectric nanogenerators (TENGs) are a promising technology for harvesting ambient mechanical energy, yet their durability is fundamentally limited by friction-induced wear at functional interfaces. Friction in TENGs is inherently paradoxical: it enables charge generation while simultaneously accelerating material degradation. This review systematically summarizes five advanced mechanical friction-reduction strategies developed to address this paradox, including rolling friction, soft contact, intermittent contact, non-contact and interface lubrication. Each friction-reduction strategy is systematically evaluated with respect to the corresponding structural design, operating mechanism and application scenarios in insulator- and semiconductor-based TENGs. Furthermore, a comparative evaluation is conducted to provide a foundational understanding of how friction-reduction methods influence the performance of TENGs and to guide future design optimization. In addition, we outlook the emerging trends toward intelligent, integrated triboelectric energy systems and present a roadmap for practical implementation and commercialization. This review offers valuable insights into the path forward for achieving highly efficient and long-term durable TENGs.

Keywords: Triboelectric nanogenerators; friction-induced wear; friction-reduction strategy; long-term durability

1. Introduction

1.1 Fundamentals of triboelectric nanogenerators (TENGs) and dual role of friction

Friction is traditionally regarded as a major cause of energy dissipation and material degradation in industrial and mechanical systems, which not only converts mechanical energy into undesired heat but also leads to wear, fatigue and eventual failure of materials and devices [1–3]. According to relevant reports, frictional energy loss accounts for one-third of global primary energy consumption. On the other hand, with the rapid development of energy harvesting technologies, friction has been redefined not solely as a detrimental phenomenon but also as a potential source of usable energy [4–8]. In recent years, triboelectric nanogenerators (TENGs) have garnered substantial research interest as a novel technology for mechanical-to-electrical energy conversion [9–13], capable of recycling the dissipated friction energy in mechanical structures or components.

Based on the composition of tribo-pair materials, TENGs can be categorized into two typical types: insulator-based TENGs (hereinafter referred to as insulator-TENGs) and semiconductor-based TENGs (also known as tribovoltaic nanogenerators, TVNGs), each of which leverages frictional interactions at different interfaces to initiate electrical output [14–18] (Figure 1a). Insulator-based TENGs function through the synergistic

effects of contact electrification and electrostatic induction. Repeated contact and separation between two dissimilar materials induce charge transfer due to differences in their electron affinities, resulting in a potential difference that drives current through an external circuit. In 2019, Wang et al. further advanced the fundamental understanding of contact electrification by proposing the electron cloud-potential well model [19], which attributes charge transfer to the overlap and subsequent separation of electron clouds at material interfaces. In this framework, electron transfer is driven by atomic-scale compression at the interface of two contacting surfaces. When the inter-surface distance is reduced below the equilibrium bond length, the overlapping electron clouds distort the initially isolated potential wells into an asymmetric double-well configuration. This deformation lowers the energy barrier and further enables electrons to tunnel from surface states of higher energy to those of lower energy. Upon separation, the transferred electrons remain trapped within their respective potential wells, resulting in one surface carrying net negative charge and the other net positive charge. This charge separation forms the basis for the electrostatic induction process that ultimately generates electrical output. Depending on the device configuration, insulator-TENGs can be divided into four typical working modes: contact-separation, lateral sliding, single-electrode and freestanding triboelectric-layer. These configurations allow flexible designs for harvesting various forms of low-frequency mechanical energy from mechanical friction, structural vibrations, human motion and environmental stimuli [20–27]. On the other hand, TVNGs based on the tribovoltaic effect have attracted extensive attention since it was first reported by Zhang et al. in 2020 [16]. The

tribovoltaic effect refers to the generation of a direct electrical current at semiconductor interfaces as a result of mechanical friction. By exploiting the intrinsic charge transport characteristics of semiconductor-semiconductor or semiconductor-metal junctions, TVNGs facilitate the excitation and directional movement of charge carriers during sliding or contact motion, enabling the direct conversion of mechanical stimuli into DC electrical output without the need for rectification circuits. Despite the remarkable progress in the development of TVNGs over the past years, a unified understanding of the internal working mechanisms has not yet been established [28,29]. Liu et al. emphasized the role of non-equilibrium carriers and tunneling through ultrathin oxide layers [30,31]. Zhang et al. attributed the DC output to the built-in electric field formed by the work function difference at the metal-semiconductor interface [16]. Lin et al. introduced a dynamic Schottky diode model, highlighting junction reformation and carrier reflection from surface states [32]. Chen et al. suggested that interfacial defect trapping in GaN-based TVNGs creates an electric field opposite to the built-in potential, which dominates the output [33]. Collectively, the emerging TENGs technology demonstrates the vast potential of converting ubiquitous frictional energy into usable electricity.

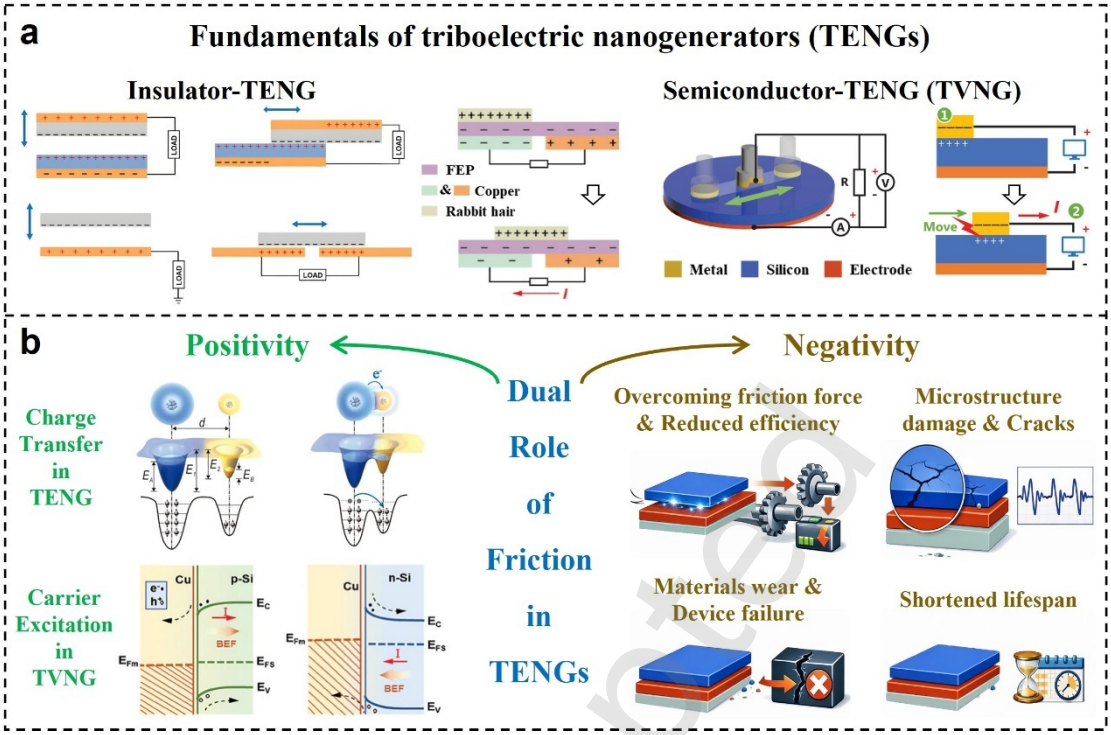

Figure 1. Fundamentals of triboelectric nanogenerators (TENGs) and dual role of friction. [14–16,19]

Although friction is the core physical basis enabling energy conversion in TENGs, it simultaneously constitutes the fundamental bottleneck limiting their conversion efficiency and long-term stability [19] (Figure 1b). As a result, friction exhibits a typical dual role in TENGs. On the positive side, friction serves as the driving force for physical contact and charge transfer. For insulator-TENGs, the applied mechanical force during friction or contact reduces the interatomic distance below the equilibrium bond length, inducing strong repulsive interactions and electron cloud overlaps between the two functional materials. This overlap forms an asymmetric double-well potential that lowers the energy barrier for electron transition, facilitating the charge transfer and further generating the electric output in external circuit. Without sufficient friction-induced compression, the necessary atomic-scale interactions for contact electrification would not occur, rendering energy generation ineffective. As to TVNGs, the motional

friction between metal-semiconductor interface or semiconductor-semiconductor interface excites electron-hole pairs. Simultaneously, the friction-induced interfacial electric field facilitates the directional separation of these carriers, allowing electrons and holes to move toward opposite electrodes. This process results in a direct current output in the external circuit. Without sufficient friction, neither carrier excitation nor effective separation would occur. However, on the negative side, friction is a critical factor detrimental to both the output performance and operational durability of TENGs. A portion of the input mechanical energy is inevitably consumed to overcome interfacial friction, thereby reducing the overall energy conversion efficiency. Moreover, repeated frictional interaction leads to progressive wear, surface roughening and fatigue-induced crack formation, especially in micro-nano-scale structures. Such phenomena cause irreversible deterioration of the effective contact area, accompanied by a reduction in triboelectric charge density, ultimately causing output attenuation and device failure over extended operation cycles.

To better clarify the dual nature and underlying patterns of friction in TENGs from a tribological perspective, it is of vital importance to establish the intrinsic coupling relationships among charge density, contact pressure, frictional power consumption and wear rate. we conducted a concise framework to clarify the coupling among these key parameters. Specifically: : (i) the surface charge density (σ) is strongly dependent on the real contact area and contact pressure, typically increasing with contact force but approaching saturation due to limited effective contact; (ii) frictional power dissipation can be expressed as $P_f \propto \mu \cdot F_N \cdot v$, where μ is the friction coefficient, F_N is the

normal force, and v is the sliding velocity; (iii) the wear rate is generally correlated with frictional energy dissipation and material properties, following classical tribological laws; (iv) excessive wear leads to surface degradation and material transfer, which in turn reduces effective charge density and destabilizes output performance. These relationships indicate a strong intrinsic coupling: increasing contact pressure enhances charge generation but also increases frictional dissipation and wear, leading to a trade-off between electrical output and mechanical durability. However, current studies mainly address these factors separately or through simplified models, a unified and quantitative framework that simultaneously integrates charge generation, frictional dissipation and wear evolution under different material systems and operating conditions is still lacking. Thus, establishing a universal multiphysics coupling model remains a critical challenge in the TENG field, and future work should focus on bridging tribology and electrostatics to achieve predictive design of high-performance and durable systems. In general, while friction is fundamental to the energy conversion of TENGs, it also imposes significant constraints on their efficiency and operational lifespan. This intrinsic duality highlights the pressing need for mechanical friction-reduction strategies, which can effectively manage and mitigate friction-induced losses and enable stable, durable and high-performance TENGs.

1.2 Advanced mechanical friction-reduction strategies in TENGs

According to detailed analysis in the previous section, friction not only enables charge generation in insulator-TENGs and carrier excitation in TVNGs, but also accelerates wear, fatigue and interfacial degradation, ultimately compromising output

stability and lifespan of TENGs. As TENGs find increasingly broad applications in distributed sensing, wearable electronics and low-power IoT systems, there is a growing demand for design strategies that can mitigate friction-induced damage without disrupting the underlying energy conversion mechanisms. The challenge lies in keeping sufficient interfacial interaction to drive charge transfer, while minimizing the physical wear and energy loss typically associated with traditional contact or slide friction. To address this issue, considerable research efforts have been devoted to developing mechanical friction-reduction strategies in recent years [34–46] (Figure 2). The mechanisms by which mechanical friction-reduction strategies in TENGs enhance energy harvesting stability and efficiency can be elucidated from the following perspectives: (1) Reduction of frictional energy loss: By minimizing the wastage of input mechanical energy, a greater proportion of the input energy can be converted into electrical energy; (2) Suppression of interfacial air breakdown: This preserves more frictional charges for electrostatic induction; (3) Maintenance of effective contact area: By reducing wear, a high surface charge density and stable output can be sustained.

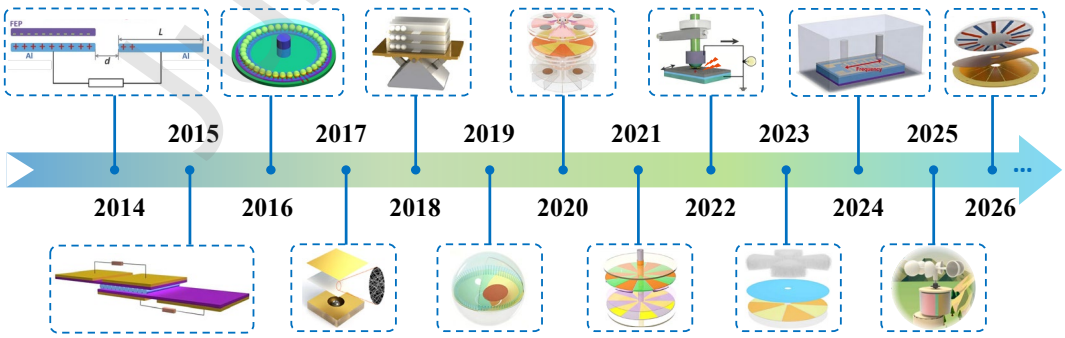

Fig. 2 The development of mechanical friction-reduction strategies in TENGs [34–46].

Recent advances in structural and material engineering have yielded five representative mechanical friction-reduction strategies to reduce wear in TENGs:

rolling friction, soft contact, intermittent contact, non-contact and interface lubrication [47,48]. Rolling friction structures reduce tangential shear stress by transforming sliding motion into rolling motion, thereby significantly lowering the friction coefficient. Soft contact designs incorporate elastomers or other flexible materials at friction interface to distribute pressure more evenly and delay fatigue failure. Intermittent contact architectures introduce periodic separation between active layers, reducing the accumulation of frictional wear during operation. Non-contact structures exploit electrostatic induction to realize charge transfer without direct physical contact, thus achieving near-zero wear. Interface lubrication introduces physical or chemical lubricants to reduce friction at the interface while preserving sufficient electrical interaction. Several previous reviews have addressed durability challenges in TENGs, but most have focused on the wear resistance or surface charge retention of functional materials, including material selection, structural optimization and power management. In contrast, this review provides a systematic and comparative analysis of mechanical friction-reduction strategies from an engineering tribology perspective. Specifically, it categorizes and compares five representative strategies including rolling friction, soft contact, intermittent contact, non-contact, and interface lubrication from both mechanical and functional standpoints. Sections 2 to 6 are dedicated to the individual discussion of each approach, including their working principles, representative device structures, performance characteristics and application scenarios. Section 7 presents a comparative evaluation of the strategies across key performance metrics such as output retention, cycling stability and structural complexity. Finally, Section 8 outlines future

directions toward the integration of multiple strategies, intelligent system design and roadmap considerations for practical deployment. Through this review, we aim to provide a practical foundation for designing next-generation TENGs with enhanced durability and energy conversion efficiency.

2. Rolling friction for enhancing efficiency and durability of TENGs

Rolling friction, essentially static in nature, provides an effective route to reduce interfacial wear and enhance device durability in TENGs [49–53]. Unlike sliding contact, which suffers from severe abrasion and heat generation, rolling friction minimizes energy loss and enables long-term stable operation.

Lin et al. first introduced a rolling freestanding TENG in 2015 [36], employing steel rods sandwiched between FEP films to realize rolling-induced electrification, as shown in Figure 3a. This architecture achieved an open-circuit voltage of 425 V and a short-circuit current density of 5 mA/m^2 for each pair of output terminals, together with a maximum power density of 1.6 W/m^2. In addition, the instantaneous conversion efficiency of up to 55% was achieved, while SEM characterization confirmed minimal surface wear (Figure 3b), highlighting the robustness of rolling friction. Building on this concept, Tang et al. proposed a rolling belt-based TENG that transformed sliding friction into interface static friction [49] (Figure 3c). By enlarging the contact area through a belt structure and adopting the self-excitation method (Figure 3d), the device achieved about 3.8 times higher output compared to rod-based counterparts, sustained over 4.1 million cycles with exceeding 98.5% retention, and reached the highest charge density (170 $\mu C/m^2$) among sliding-free TENGs. What's more, the significantly

reduced weight of the device (6.42 μg/g per 10k cycles) underscores its durability. Fu et al. reported a rolling TENG based on a mechanical planetary structure [50], as depicted in Figure 3e. The planetary rolling configuration provided multiple dynamic contact points, ensuring both mechanical stability and efficient charge transfer during continuous rotation. The device exhibited a low starting wind speed of 2 m/s and achieved an open-circuit voltage close to 240 V together with a short-circuit current of 25.18 μA at 5 m/s. Moreover, it maintains stable output responses even after 6 million continuous operation cycles (Figure 3f). Zhu et al. introduced a regenerative motion transmission (RMT) architecture for triboelectric-electromagnetic hybrid nanogenerators [46], utilizing dual-cylinder rolling friction to transform sliding friction into coaxial rolling friction, as shown in Figure 3g. The RMT-based system achieved lower cut-in wind speeds (2.5 m/s) and retained 98.9% output after 100 thousand cycles (Figure 3h), demonstrating remarkable friction reduction and operational stability. Above studies establish rolling friction as a powerful structural strategy to mitigate wear, prolong device lifespan and enable stable high-performance output in diverse triboelectric systems. Building upon these design principles, diverse applications and operational outcomes of rolling-friction-based TENGs have been developed and reported over the past years.

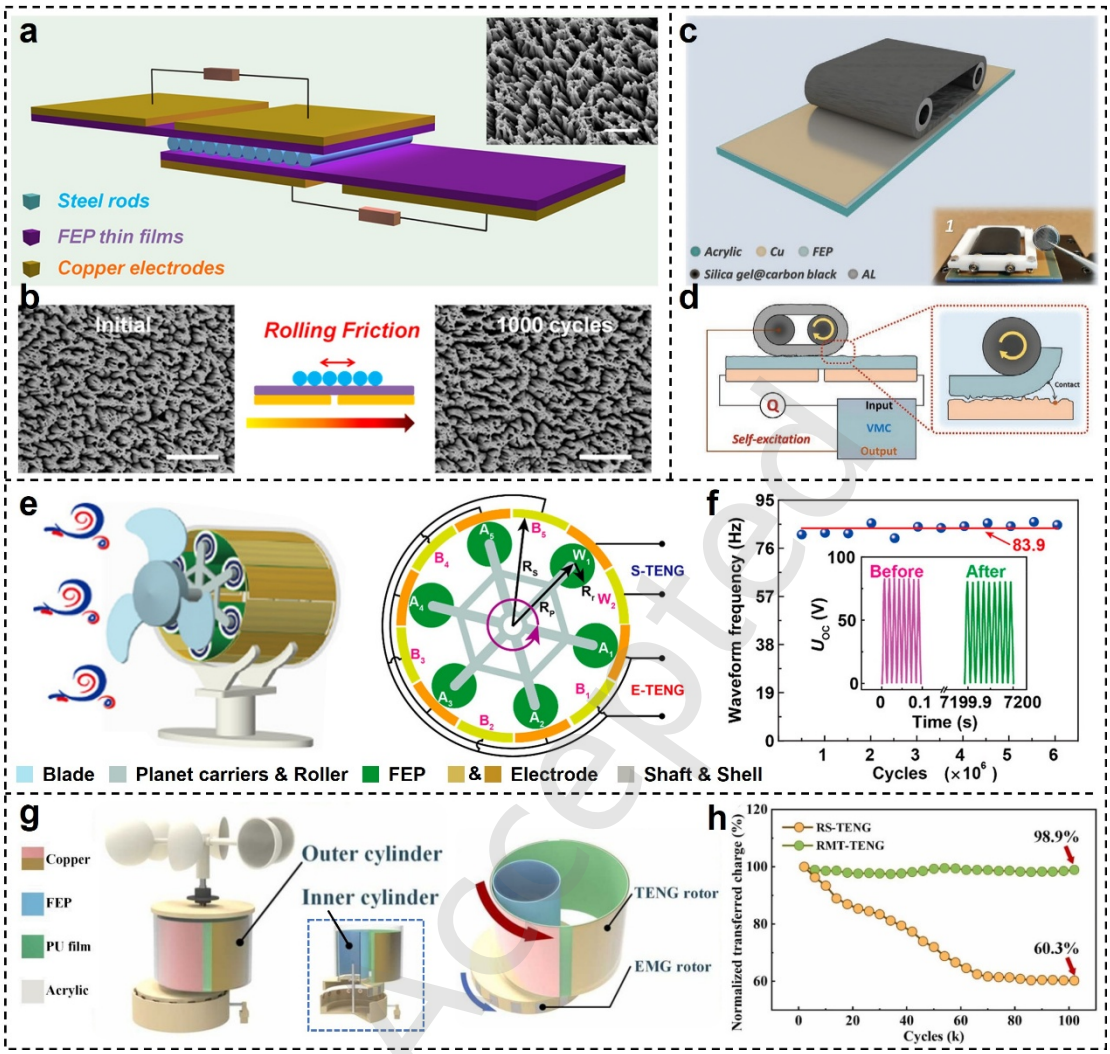

Figure 3. Structural designs based on rolling friction in TENGs. (a) Structural diagram of the rolling freestanding TENG; (b) Comparison of surface morphology after 1000 cycles[36]; (c) Structural of the rolling belt-based TENG and (d) its diagram of self-excitation method [49]; (e) Schematic of planetary structure-based rolling TENG and (f) its stability test [50]; (g) Structural diagram of the regenerative motion transmission -based hybrid generator; (h) Normalized charge outputs of regenerative motion transmission TENG and rotary sliding TENG versus working cycles [46].

One representative application of TENGs lies in environmental energy harvesting and distributed sensing in unstable and complex scenarios [54–57]. Fu et al. reported a planetary rolling TENG system that converts breeze-driven rotational motion into

electrical energy [50], as depicted in Figure 4a. Benefitting from the planetary rolling friction, the self-powered system operates at ultra-low startup wind speeds and maintains long-term stability, enabling continuous energy harvesting while simultaneously functioning as an active wind-speed sensor (Figure 4b). Integrated with power management unit and wireless transmission modules, it enabled stable operation of a self-powered anemometer (Figure 4c), illustrating its potential for autonomous environmental monitoring and IoT-based sensing networks. Xi et al. developed a rolling TENG array incorporating a ternary dielectric configuration for applications in ocean energy harvesting and distributed environmental monitoring. [53] (Figure 4d-e). The rolling TENGs embedded within buoy structures exploit wave-induced motion to drive PTFE balls along predefined tracks (Figure 4e), which could keep smooth motion even under low-frequency and low-amplitude excitations, significantly enhancing durability in harsh ocean conditions. At a low excitation frequency of 0.5 Hz, a four-unit TENG array charged a 10 mF capacitor to 5 V within 175 s. Meanwhile, the integrated wireless ocean sensing system realized real-time detection of pH and temperature. Another compelling application involves integrating such TENGs into mechanical structures or components for intelligent sensing and monitoring [22,58–60]. Dong et al. developed an AI-enabled bearing-structured rolling TENG where rolling balls simultaneously serve as mechanical transmission elements and freestanding triboelectric layers [52] (Figure 4f). The rolling friction between PTFE balls and interdigitated electrodes generates stable electrical waveforms that encode bearing health information. By coupling these signals with advanced signal decomposition and deep learning

algorithms, the system achieves 95.20~98.40% accuracy in diagnosing wear types, degrees (detecting minor defects down to 1-5% weight loss) and positions on rolling elements. This application leverages the unique advantage of rolling friction in preserving both mechanical integrity and signal repeatability in TENGs, enabling real-time condition assessment and digital twin integration for predictive maintenance.

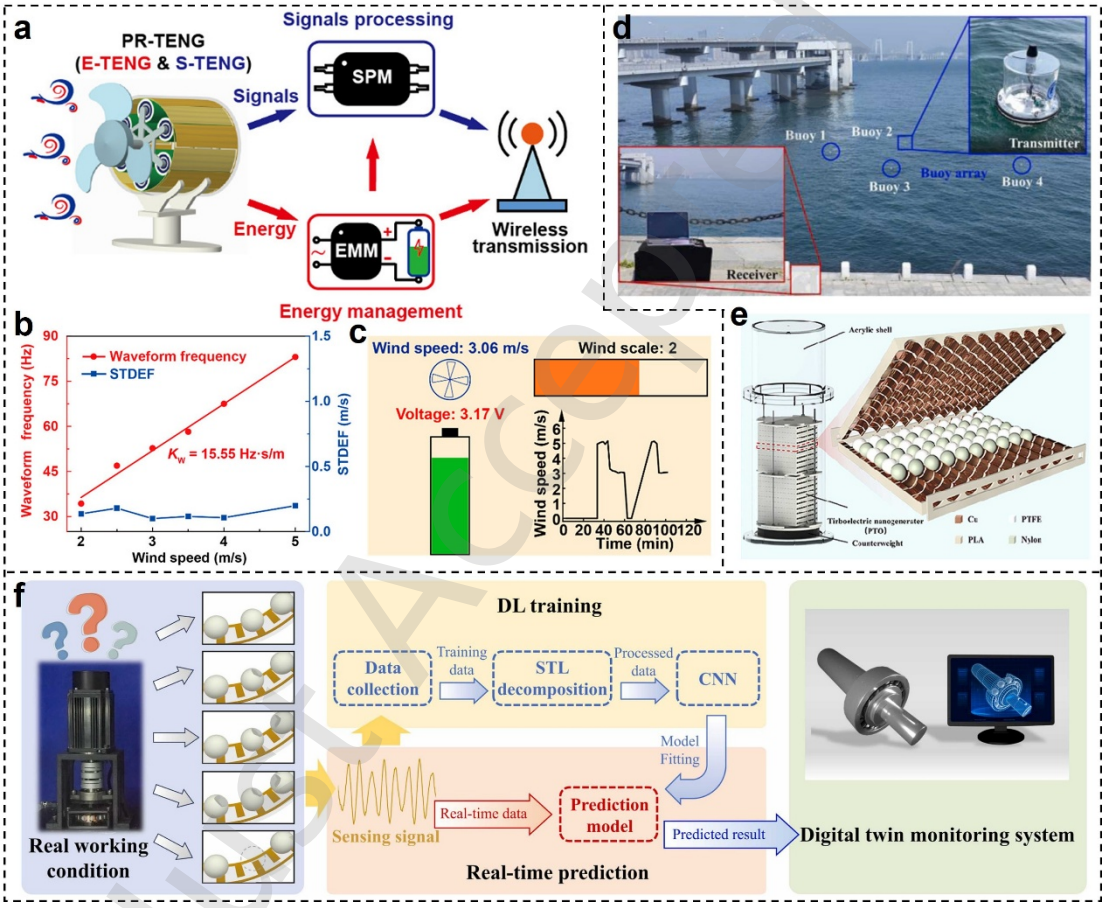

Figure 4. Applications of rolling friction in TENGs. (a) Framework of the wind-powered anemometer; (b) The waveform frequency at different wind speeds and (c) the display interface of the wireless receiving terminal [50]; (d) Ocean data collection by the ternary-dielectric rolling TENG array; (e) Structural design of the ternary-dielectric rolling TENG [53]; (f) Digital twin-oriented bearing health monitoring system [52].

3. Soft contact for enhancing efficiency and durability of TENGs

Soft-contact strategies have emerged as a versatile and unified approach to simultaneously enhance the durability and electrical output of TENGs [61–65]. As shown in Figure 5a-b, Han et al. reported a rabbit-fur based soft-contact rotary TENG [61], where the intrinsic elasticity of fur brushes markedly suppresses interfacial abrasion while maintaining efficient charge transfer. The device sustained exceeds 95% charge retention after 4.8 million cycles and achieved a mechanical-to-electrical conversion efficiency of 15.4% under breeze speeds as low as 1 m/s, enabling long-term operation in smart farming applications. Lin et al. introduced an elastic-connection and soft-contact pendulum architecture TENG [66], as depicted in Figure 5c, in which a spring-assisted pendulum structure and flexible dielectric fluff are introduced to replace rigid contact interfaces. The compliant fluff enables gentle yet effective triboelectrification, significantly mitigating material abrasion, while the elastic connection allows intermittent soft contact and predominantly non-contact operation. This configuration achieves a vibration-to-electricity conversion efficiency of 29.7% per stimulus and exhibits less than a 3% degradation in open-circuit voltage after 2 million cycles, demonstrating an exceptional trade-off between high performance and long-term durability. Yang et al. designed a ternary four-phase stacked TENG that incorporates dual-soft interfaces of polyester-fur brushes and sponge-supported PTFE/nylon films [67], as shown in Figure 5d. The compliant brush–sponge interface compresses during rotation, narrowing the gap and enhancing charge generation, while the brush replenishes dissipated charges to stabilize output. This device delivered 354%/185% higher voltages than binary/ternary controls and eliminated observable

wear after 30 thousand cycles. Cao et al. scaled the strategy to a large-area cylindrical freestanding rotating TENG with nylon/PTFE soft tribo-pairs [68] (Figure 5e). Compared with hard-contact counterparts, the soft-contact structure reduced torque consumption by an order of magnitude while maintaining a similar short-circuit current of almost 35 μA (Figure 5f). These soft-contact architectures mitigate interfacial stress and torque while maintaining effective charge transfer, thereby enabling stable output under low-grade mechanical inputs.

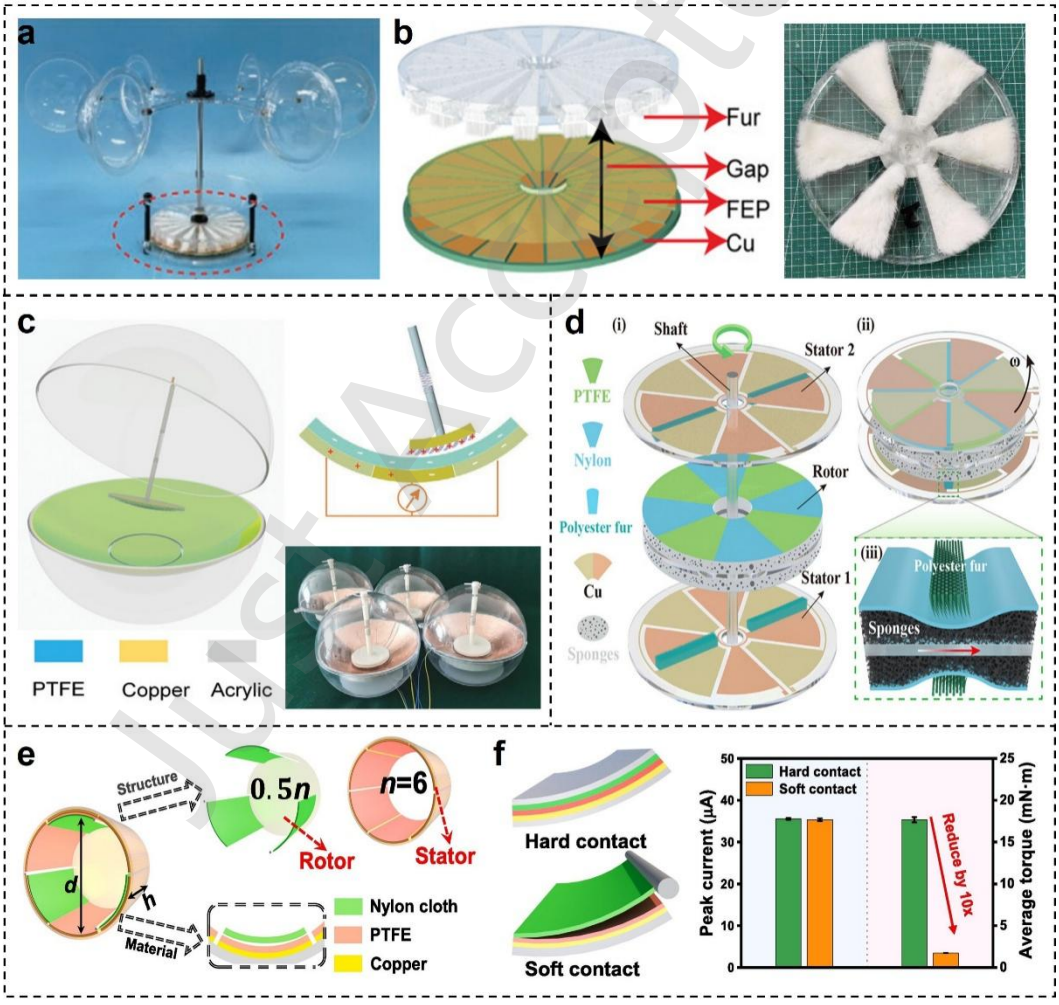

Figure 5. Structural designs based on soft contact in TENGs. (a-b) Structural diagram and physical image of the rabbit-fur based soft-contact rotary TENG [61]; (c) Structural diagram and physical image of the soft-contact pendulum architecture TENG [66]; (d) Exploded view of the ternary four-phase stacked

TENG [67]; (e) Structural diagram of the cylindrical freestanding rotating TENG and (f) its output comparison between hard contact and soft contact [68].

Zhao et al. developed a self-adaptive soft-contact ellipsoidal pendulum structured TENG that couples a rigid outer spherical shell with an internal soft liquid-balloon system filled with NaCl solution [64] (Figure 6a). The device was Integrated into a GPS wireless positioning and real-time tracking platform: the wave-driven output powered a GPS module and enabled acquisition of longitude, latitude, altitude and related location information at a computer terminal (Figure 6b-c). With rectification and series connection for voltage boosting, the system charged a 4.70 μF capacitor to 3.7 V (GPS-rated voltage) within 39.66 s at 30 MΩ, supporting scalable TENG-network deployment for mobile marine nodes. Lin et al. extended soft-contact concepts to practical blue-energy and IoT scenarios via an elastic-connection and soft-contact TENG [66], as shown in Figure 6d. The peak current of the device scaled with unit number and reached 4.4 μA for six units (Figure 6e), a self-powered temperature/humidity monitoring system for remote ocean sensing and wireless transmission was demonstrated, highlighting the role of soft contact in durability-oriented, maintenance-free deployments. Liu et al. employed soft-contact materials within a coaxial double-rotation TENG to simultaneously reduce wear and enhance power delivery [65]. Benefiting from its robust output and enhanced durability, the device was effectively deployed for electrochemical corrosion protection (Figure 6f). Metallographic observations highlighted its protective capability: unprotected steel exhibited rapid rusting within 1-2 h, whereas the TENG-protected sample showed only slight corrosion

after 6 h (Figure 6g), demonstrating its great potential in the field of cathodic protection.

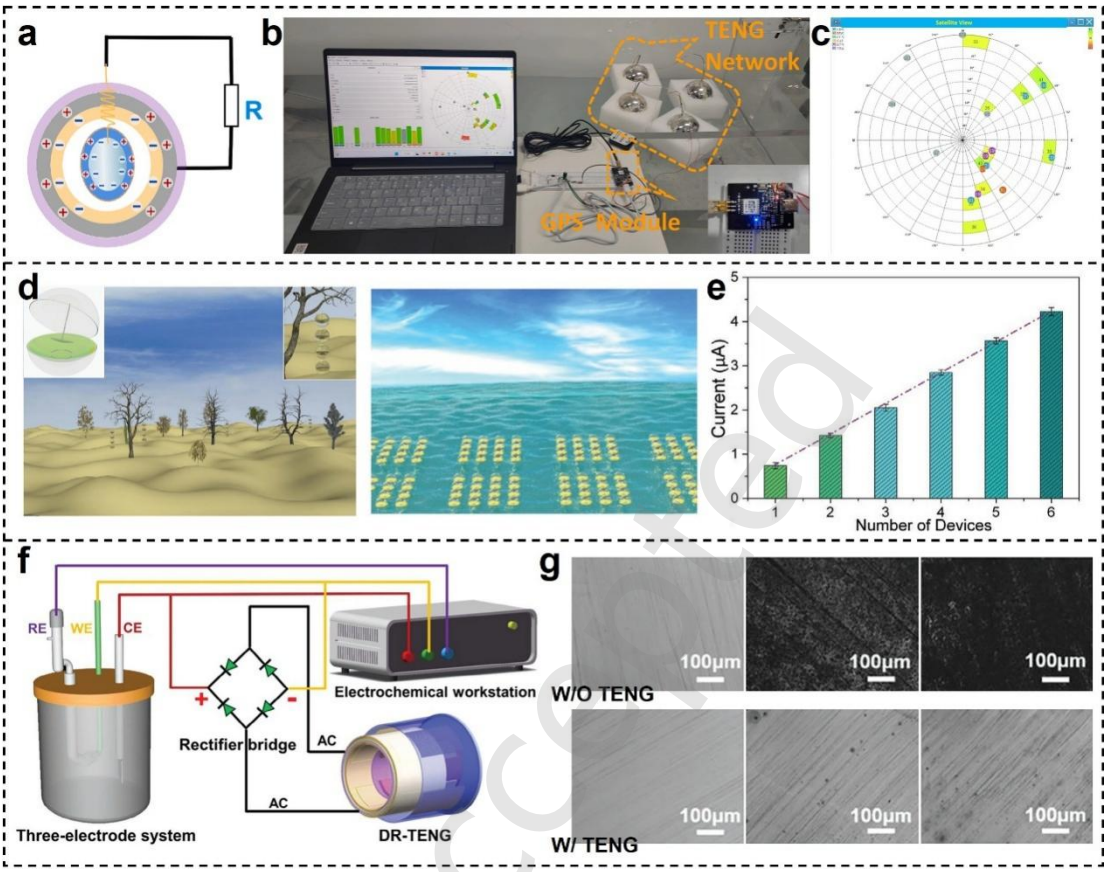

Figure 6. Applications of soft contact in TENGs. (a) Structural diagram of the pendulum-structured TENG; (b-c) Photograph of the GPS wireless positioning and real-time tracking [64]; (d) Schematic of the elastic-connection and soft contact TENG array and (e) its Output peak currents with different units [66]; (f) Schematic diagram of coaxial double-rotation TENG power supply electrochemical cathodic protection system; (g) Photos of the metallographic structure of the Q235 carbon steel with and without coaxial double-rotation TENG protection [65].

4. Intermittent contact for enhancing efficiency and durability of TENGs

Beyond static soft-contact strategies, intermittent-contact designs provide a dynamic pathway to reconcile high charge output with long-term operational stability [69–74]. As shown in Figure 7a, Chen et al. introduced a centrifugal-force-triggered freestanding TENG with automatic working mode transition [41]. At low rotational

speeds, the PU freestanding layer maintains full contact with the FEP film. When the rotational speed surpasses 225 rpm, increasing centrifugal forces cause the sliders to disengage and result in non-contact operation. This automatic transition enables the device to maintain almost 90% of its initial output after 24 hours of continuous operation. Fan et al. developed an automatic-mode-transition (AMT) triboelectric-electromagnetic hybrid generator enabled by a maglev-induced vertical oscillation of the rotor [73], as depicted in Figure 7b-c. The intermittent-contact regime at low wind speeds allows brief sliding between FEP and Cu electrodes to replenish dissipated charges, while the device naturally enters non-contact operation as rotation accelerates, mitigating frictional drag and wear. The hybrid starts from 2.4 m/s and the TENG unit achieves a maximum weight power density of 449.5 mW/kg with an energy conversion efficiency of around 12.3% at 5.0 m/s. After 10 days of operation, the AMT mode demonstrated a superior output retention of 82%, significantly outperforming the non-contact mode (36%) and contact mode (10%). Luo et al. introduced a travel-controlled TENG in a breeze-driven triboelectric–electromagnetic hybrid generator [70], where a gear train transmits motion to a tunable cam switch that periodically raises/lowers the stator shaft (Figure 7d). This programmed contact to non-contact alternation decouples charge regeneration from continuous sliding: the convex cam segment enforces short contact for tribo-charge refresh, followed by a lifted non-contact interval to suppress abrasion (Figure 7e). Stable mode transition can be realized at 3 m/s, and the electrical outputs maintain 90% after 80 h continuous operation (1.92 million cycles). Fu et al. proposed a charge-excited, mode-adjustable rotational hydrodynamic TENG

integrating a Main-TENG and an Excited-TENG [71], as shown in Figure 7f. A centrifugal driving layer with steel balls enables automatic switching: contact at low rotation for strong triboelectrification and separation at high speed to reduce friction (Figure 7g). Meanwhile, a gear set lowers the Excited-TENG speed to alleviate wear (Figure 7h), and rectified Excited-TENG output injects charges into the Main-TENG to boost charge density. The device retains 94% output after 72 thousand cycles (vs 30% for normal contact mode) and can light 944 LEDs.

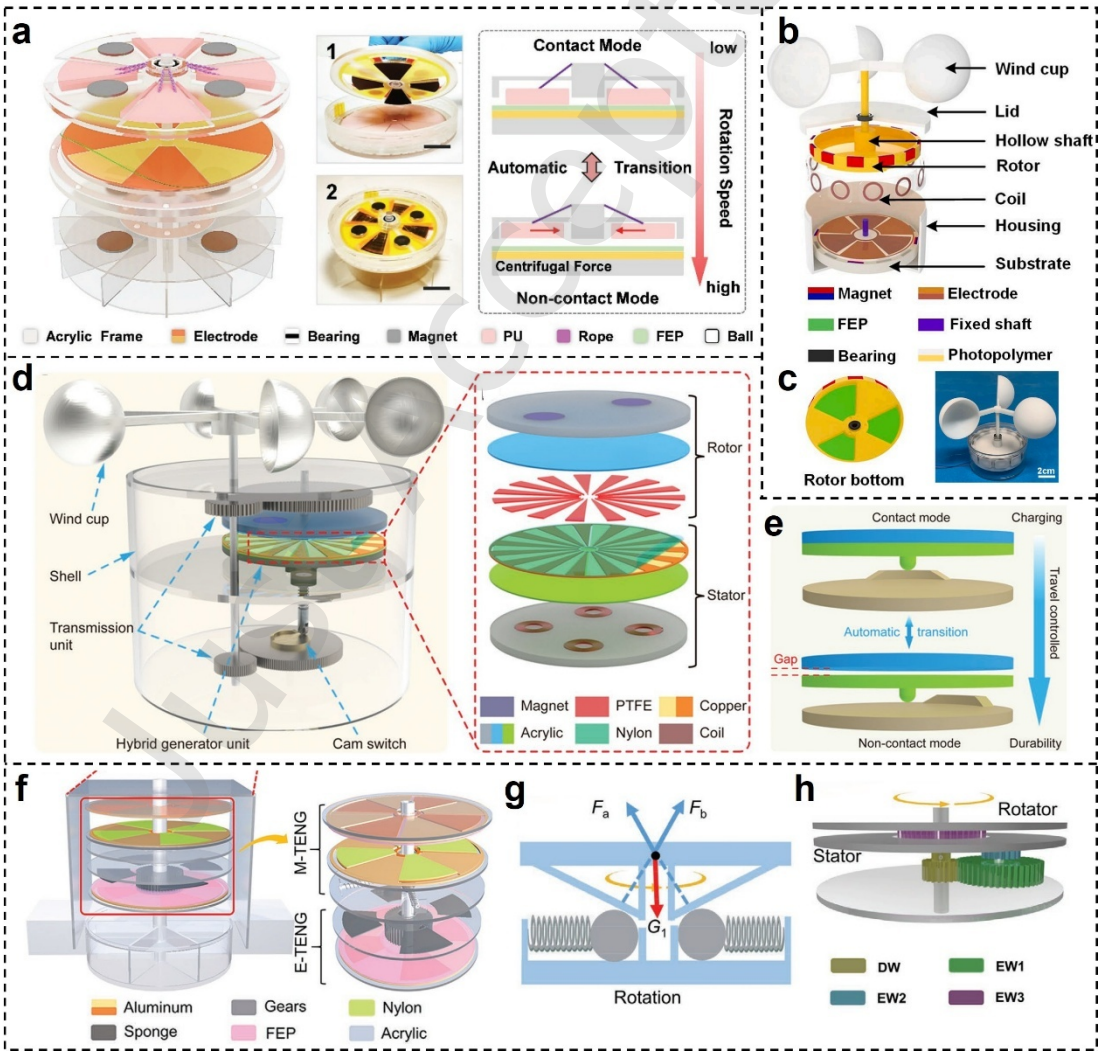

Figure 7. Structural designs based on intermittent contact in TENGs. (a) Structure of the centrifugal-force-triggered freestanding TENG [41]; (b) Exploded view of the AMT hybrid generator and (c) its

physical image [73]; (d) Structure of the hybrid device; (e) Illustration of the automatic working mode transition [70]; (f) Architectural diagram of the charge-excited, mode-adjustable rotational hydrodynamic TENG; (g) Force analysis of the rotator and (h) diagram of the gear system [71].

Over the past years, the intermittent contact-based TENGs have widely been utilized in harvesting environmental energy with excellent output and durability. Benefitting from the outstanding output performance and durability of the charge-excited, mode-adjustable rotational hydrodynamic TENG, Fu et al. utilized it to capture hydrodynamic energy from rivers or streams in the wild (Figure 8a) [71], providing a convenient and maintenance-free energy supply solution for wild IoT and intelligent forest fire monitoring. In application demonstrations, the peak power of the TENG achieves 19 mW at a rotational speed of 420 rpm, the harvested hydrodynamic energy rapidly charged commercial capacitors (Figure 8b) and lit 944 green LEDs in series with high brightness (Figure 8c). Furthermore, the managed output of the TENG could deliver adequate electrical power to operate two commercial hydro-thermographs in parallel together with a commercial infrared light alarm module, demonstrating strong power delivery under continuous water-flow excitation and highlighting an intermittent-contact pathway to long-life, self-powered sensing and warning systems in remote stream/river environments. Lin et al. designed a blue-energy harvesting device that incorporates a rotational TENG arranged in a radial array and coupled to a wave-excited transmission mechanism [69], as shown in Figure 8f. During each wave impact, a flabellum–spring trigger briefly forces the rotor into contact with the PTFE/electrode stator for charge generation. The charged rotor then swings freely within a gap,

producing electrostatic-induction output without sustained rubbing. The output can persist for almost 22 s after one excitation and reaches a maximum power of 74 μW at a matched load of 100 MΩ (Figure 8g-h). As shown in Figure 8i, each unit is rectified and then connected in parallel to form TENG arrays for large-scale energy harvesting and sensor-node powering for system-level deployment. As demonstrations, a single device continuously illuminated the "OCEAN" sign composed of 55 LEDs and powered a digital thermometer, indicating the capability of the TENG in self-powered systems at a large scale.

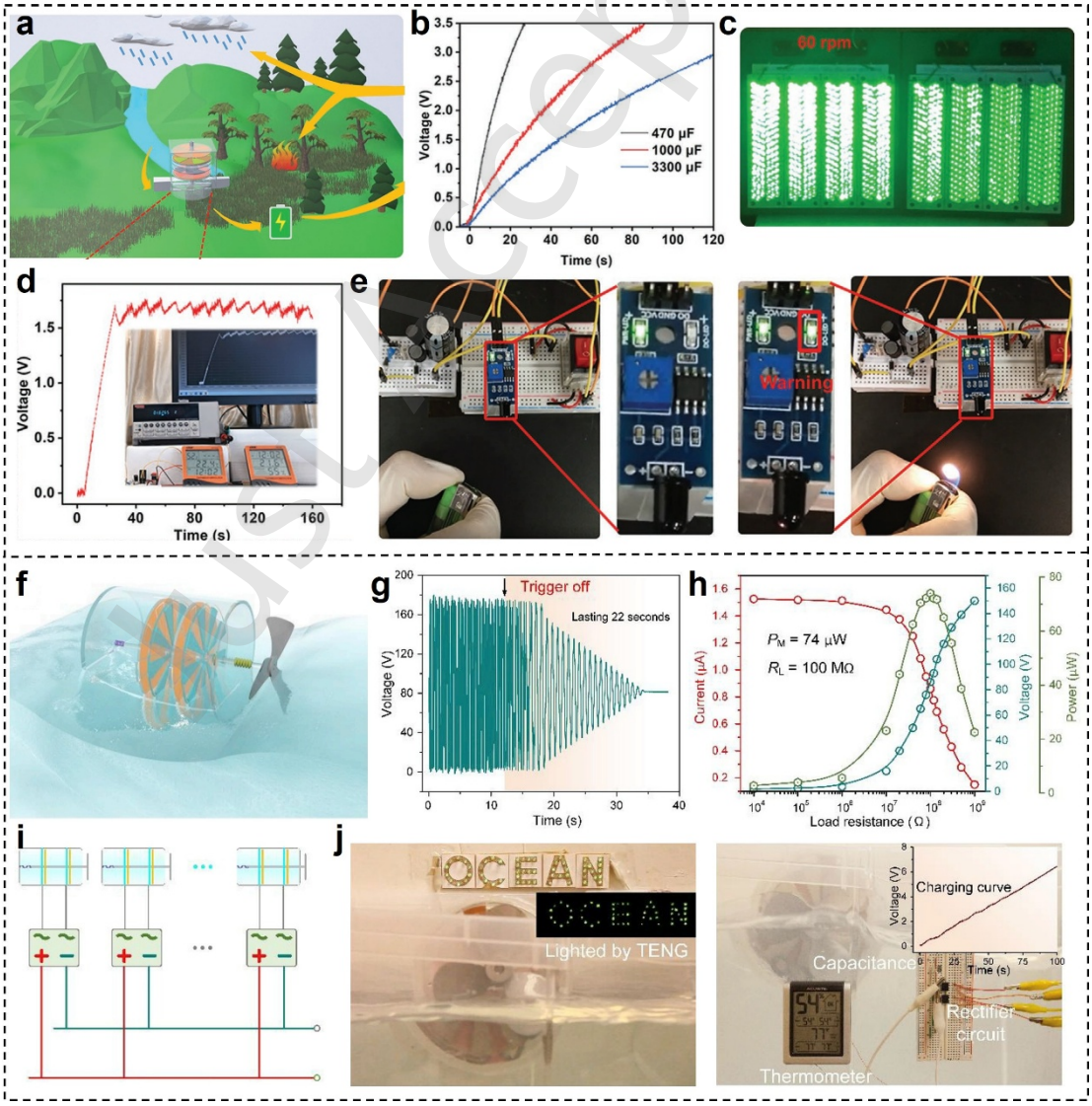

Figure 8. Applications of intermittent contact in TENGs. (a) Application scenario of the hydrodynamic TENG; (b) Charging voltage on various capacitors; (c) Image of 944 LEDs lighted by the hydrodynamic TENG; (d) Voltage variation of a 1 mF capacitor while powering two parallel-connected commercial hydro-thermographs; (e) Intermittent monitoring of a commercial infrared light alarm module [71]; (f) Schematic illustration of the radial-arrayed rotational TENG in water; (g) Lasting time of the output voltage for a trigger; (h) Output performance of the TENG; (i) Schematic of the circuit for the TENG array; (j) Image of the TENG to power a serial LED and a thermometer [69].

5. Non-contact for enhancing efficiency and durability of TENGs

Non-contact strategies eliminate direct interface wear by maintaining a finite gap between tribo-layers, thereby enabling friction-free and long-lifetime operation [75–81]. Long et al. reported a non-contact self-excited sliding TENG firstly in 2021 [42] (Figure 9a), in which the rotator-stator pair is combined with a voltage-multiplying circuit to build a self-excitation loop that boosts the effective surface charge without relying on persistent solid–solid rubbing, as depicted in Figure 9b. Compared to a traditional non-contact TENG, the proposed device delivered a 5.46 times enhancement in effective charge density (reaching 71.53 $\mu C/m^2$). In addition, the output performance of the device remained stable and even slightly improved after 100 thousand cycles of stability testing, which confirms the device's robust durability while providing an effective solution to the inherently low output of non-contact sliding TENGs. Fu et al. proposed a coaxial non-contact rotational TENG enabled by bearing charge pumping [79] (Figure 9c), where a pumping TENG in freestanding mode is built on a rolling ball bearing and coupled to an output TENG via a voltage-multiplying circuit and buffer

capacitor (Figure 9d). The low charge generated by the pumping TENG is accumulated and injected into the non-contact output TENG, simultaneously realizing ultralow mechanical wear and high output performance. This architecture achieved a transferred charge of 110.61 nC and 32-fold instantaneous power enhancement over the pumping TENG while maintaining 95% charge retention after 15 days (6.4 million cycles). Lei et al. introduced a largely enhanced non-contact TENG by introducing a high-insulation dielectric-oil gap and a charge-excitation architecture [77], as shown in Figure 9e. The non-contact TENG supports two charge-excitation methods (Figure 9f), the effective charge density reaches 212.5 $\mu C/m^2$ with an 8.37 μA stable current and a 17.105 mW peak power in the self-charge excitation route. Chen et al. developed a non-contact bidirectional spinning oscillating float-type TENG [80], in which a planetary-gear-enabled counter-rotation mechanism converts low-frequency, multidirectional vertical wave motions into high-frequency rotational electrification while maintaining a non-contact interface to eliminate frictional wear, as shown in Figure 9g-h. At 0.5 Hz, the oscillating float-type TENG outputs a peak power of 93.5 mW with an average volumetric power density of 31.3 W/m^3, and it shows no significant degradation after 5.68 million cycles, demonstrating the durability advantage of gap-regulated non-contact operation.

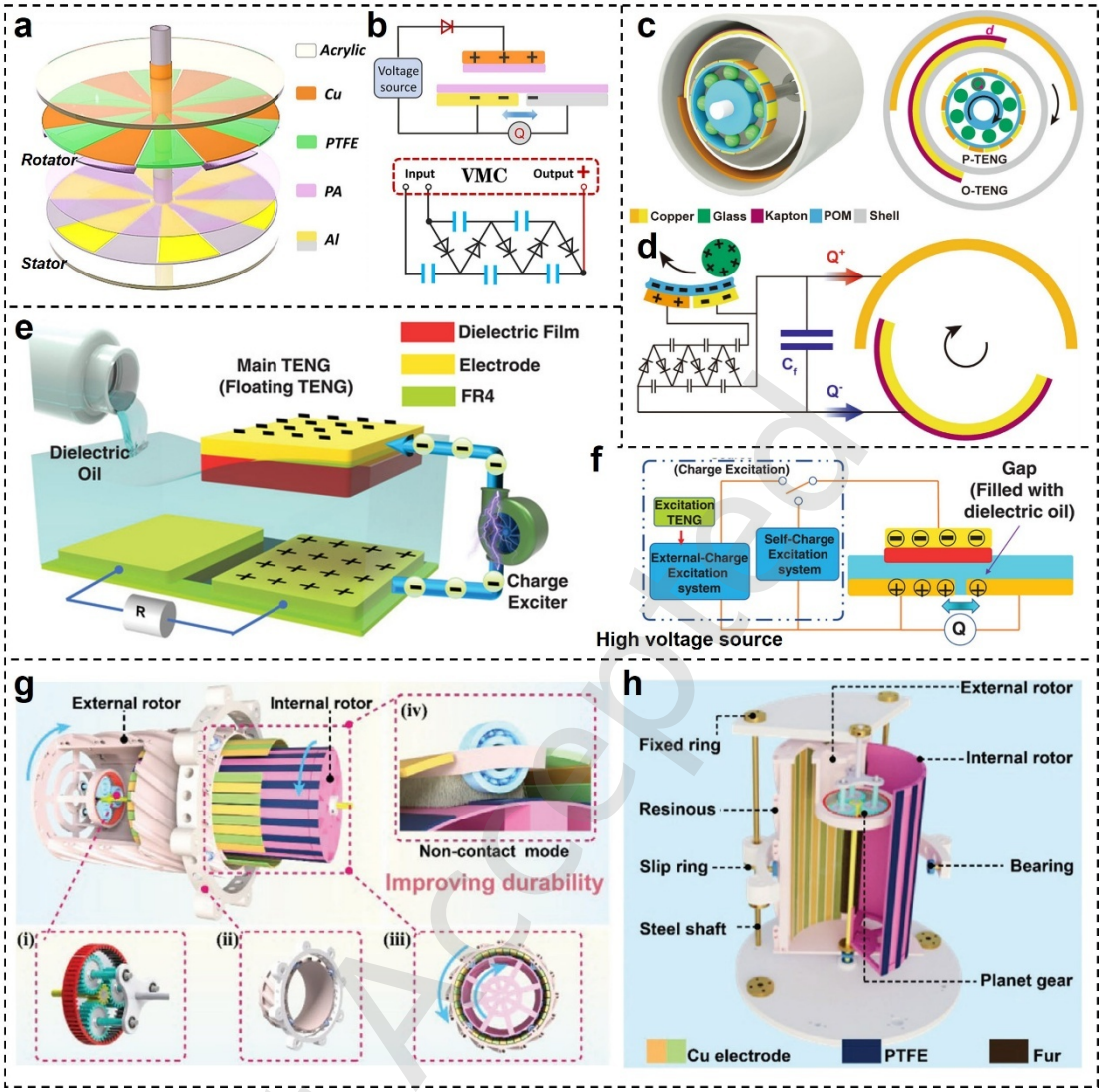

Figure 9. Structural designs based on non-contact in TENGs. (a) Structural diagram of the rotary non-contact self-excited sliding TENG and (b) its simplified working circuit schematic [42]; (c) Structural schematic of the non-contact rotational TENG and (d) its working principle [79]; (e) Schematic of non-contact TENG with high electric insulation strategy and (f) its two charge-excitation modes [77]; (g) Schematic of the 3D structure of the oscillating float-type TENG and (h) its detailed components [80].

Non-contact operation in triboelectric energy devices fundamentally eliminates direct interfacial friction by maintaining a constant gap between tribo-layers during energy conversion. This way not only avoids material wear but also opens distinct avenues for applications where durability and sustained output are paramount. In the

representative blue-energy scenario, Chen et al. integrated a non-contact oscillating float-type TENG into a self-powered smart marine ranching platform to realize both automatic feeding and water-quality monitoring [80], as shown in Figure 10a. The non-contact bidirectional spinning design converts irregular, low-frequency vertical wave motions into a stable electrical source with a peak power of 93.5 mW at 0.5 Hz. A 22 mF capacitor can be charged from 0 to 5 V within 56 s by oscillating float-type TENG with PMC, and the stored energy is then used to trigger an electronic switch for smart feeding after charging to 6.0 V (Figure 10b). In addition, the switch was activated to power the water quality monitoring system when the capacitor is charged to 5.0 V, and then the TDS, pH, and temperature data would be transmitted to a mobile terminal (Figure 10c-d), demonstrating its great value in marine smart aquaculture and distributed monitoring. Beyond energy supply, non-contact triboelectrification is also leveraged for condition monitoring in rotating machinery. Ying et al. developed a non-contact triboelectric misalignment detection sensor and combined it with deep learning for real-time quantitative evaluation [81], as shown in Figure 10e-f. In this scheme, rotor misalignment modulates the electrostatic induction process, and the voltage signal is adopted as a direct metric that is less vulnerable to environmental noise than conventional vibration measurements. Leveraging a ResNet18-1D model and high-fidelity sensing data, the system realized misalignment identification with over 96% accuracy, while achieving a detection resolution and measurement precision of 0.05 mm. A LabVIEW-based platform enables real-time visualization and automated inference (Figure 10g), highlighting the practicality of integrating non-contact

triboelectric sensing with data-driven algorithms for online, non-invasive misalignment diagnostics in rotating machinery.

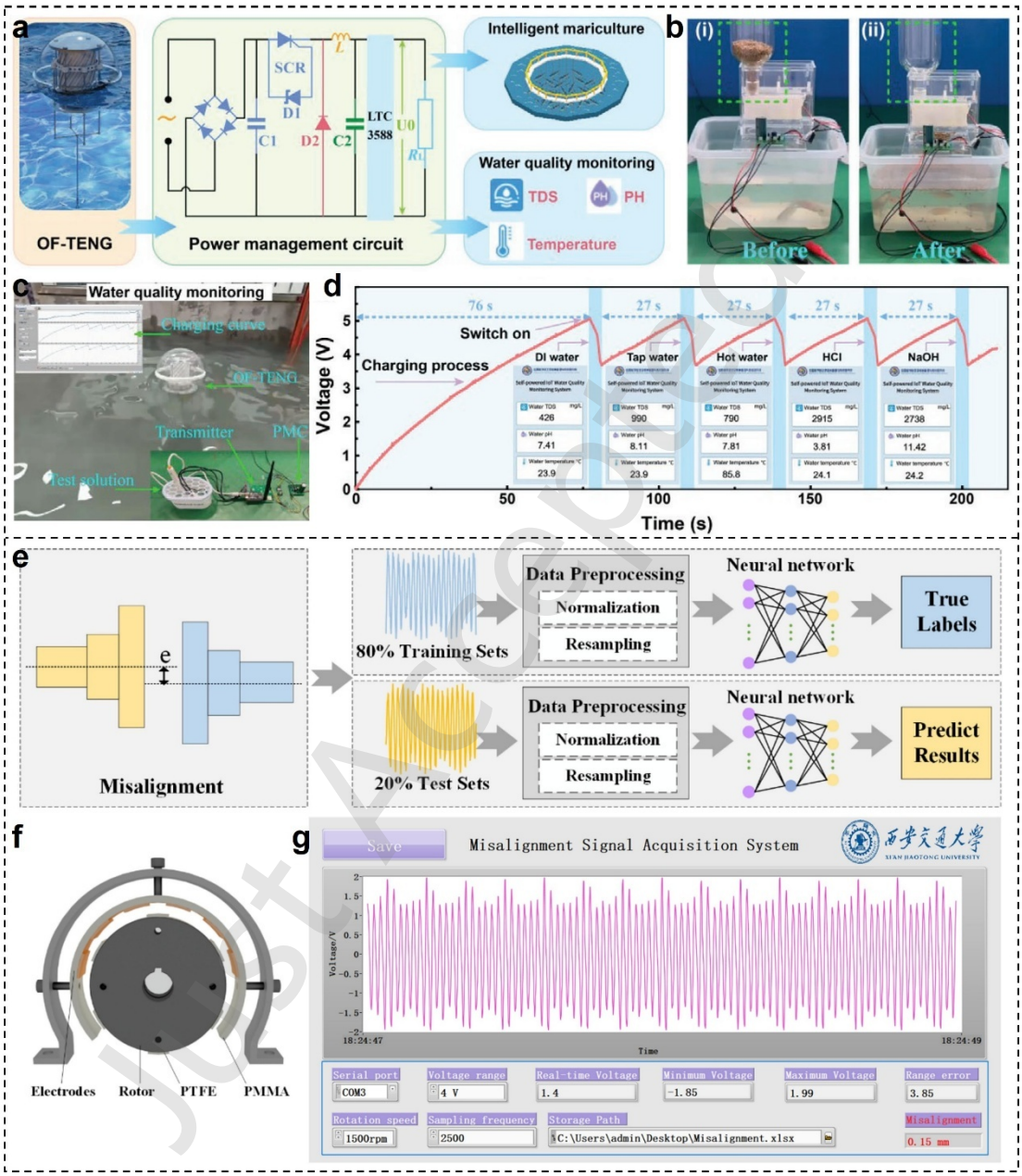

Figure 10. Applications of non-contact in TENGs. (a) Schematic of TENG-based self-powered intelligent mariculture and wireless water quality monitoring system; (b) Graph of feeding feed to fish before and after the electronic switch is turned on; (c) Photos of self-powered water quality monitoring system; (d) Working voltage variation of the self-powered wireless water quality monitoring system [80]; (e) Overview of the ResNet18-1D-based training and testing process for sample data and (f) the triboelectric

misalignment detection sensor; (f) Human‐machine interface for misalignment signal acquisition and analysis [81].

6. Interface lubrication for enhancing efficiency and durability of TENGs

The four friction-reduction strategies discussed above achieve wear reduction through adjustments and designs of mechanical structures. In contrast, the interface lubrication strategy involves introducing different lubricating materials at the functional interface of TENGs. By preventing direct interaction between the friction pair materials, it reduces the interfacial friction coefficient, alters the interfacial lubrication state and thereby achieves friction-reduction and anti-wear effects. Furthermore, introduction of suitable lubricating materials can improve triboelectric output by suppressing air breakdown and enhancing interfacial charge density [45,82–85]. Zhou et al. proposed an interface liquid-lubrication strategy for sliding-mode TENGs [86], where a thin lubricant layer fills the micro-gap and simultaneously increases the breakdown field requirement and lowers the local electrostatic field (Figure 11a–b), suppressing interfacial air breakdown and charge loss. This enables more effective charge collection via electrostatic induction and controlled breakdown, and applicable to both AC and DC sliding TENGs. Consequently, the lubricated device delivers an exceeding 50% enhancement in maximum power density to 3.45 $W/m^2/Hz$, together with excellent durability beyond 500 thousand cycles (Figure 11c). Wu et al. systematically evaluated liquid lubrication in a reciprocating sliding TENG [87] (Figure 11d), in which the lubricant is introduced before testing to regulate the contact state and monitor friction/wear concurrently with electrical outputs. They found that properly selected

low-viscosity/appropriate-permittivity liquids (e.g., squalane) can maintain effective solid-solid contact while excluding air, inhibit transfer-film formation and thus boost triboelectric outputs (Figure 11e). In addition, the service life is remarkably extended with no detectable wear after 36 thousand cycles, while the open-circuit voltage and short-circuit current exceed 3 times than those of the dry case, as well as the friction force decreases to 17-46% of the unlubricated level. Qiao et al. incorporated a water-based graphene oxide lubricant into TVNGs [88] (Figure 11f), forming a sliding interface between a copper-supported monolayer graphene layer and a silicon substrate. The lubricant here enhances interfacial lubrication to minimize wear while concurrently increasing charge-carrier density at the sliding surface to boost the tribovoltaic DC output (Figure 11g). Consequently, the lubricated TVNG delivers a peak current density of around 775 mA/m^2 and a transferred charge density of 31 mC/m^2. Moreover, it retains 95% of its electrical output after 30 thousand cycles, demonstrating the feasibility of liquid-assisted lubrication in enhancing both DC output and durability. Wang et al. demonstrated a macroscopic liquid-superlubric TENG based on a solid-liquid-solid configuration (PTFE ball / lubricating oil / ITO-coated glass) [89], as shown in Figure 11h, where mixed lubrication (boundary & hydrodynamic) drives the friction coefficient into the superlubricity regime. As shown in Figure 11i, the device simultaneously enhanced open-circuit voltage and short-circuit current by 53.0% and 58.4%, respectively, while reducing the friction coefficient to about 0.0025 (99.1%) and the wear rate to about 0.76×10^{-7} $mm^3/N\cdot m$ (99.993%), resolving the long-standing high-output/low-friction dilemma in TENGs.

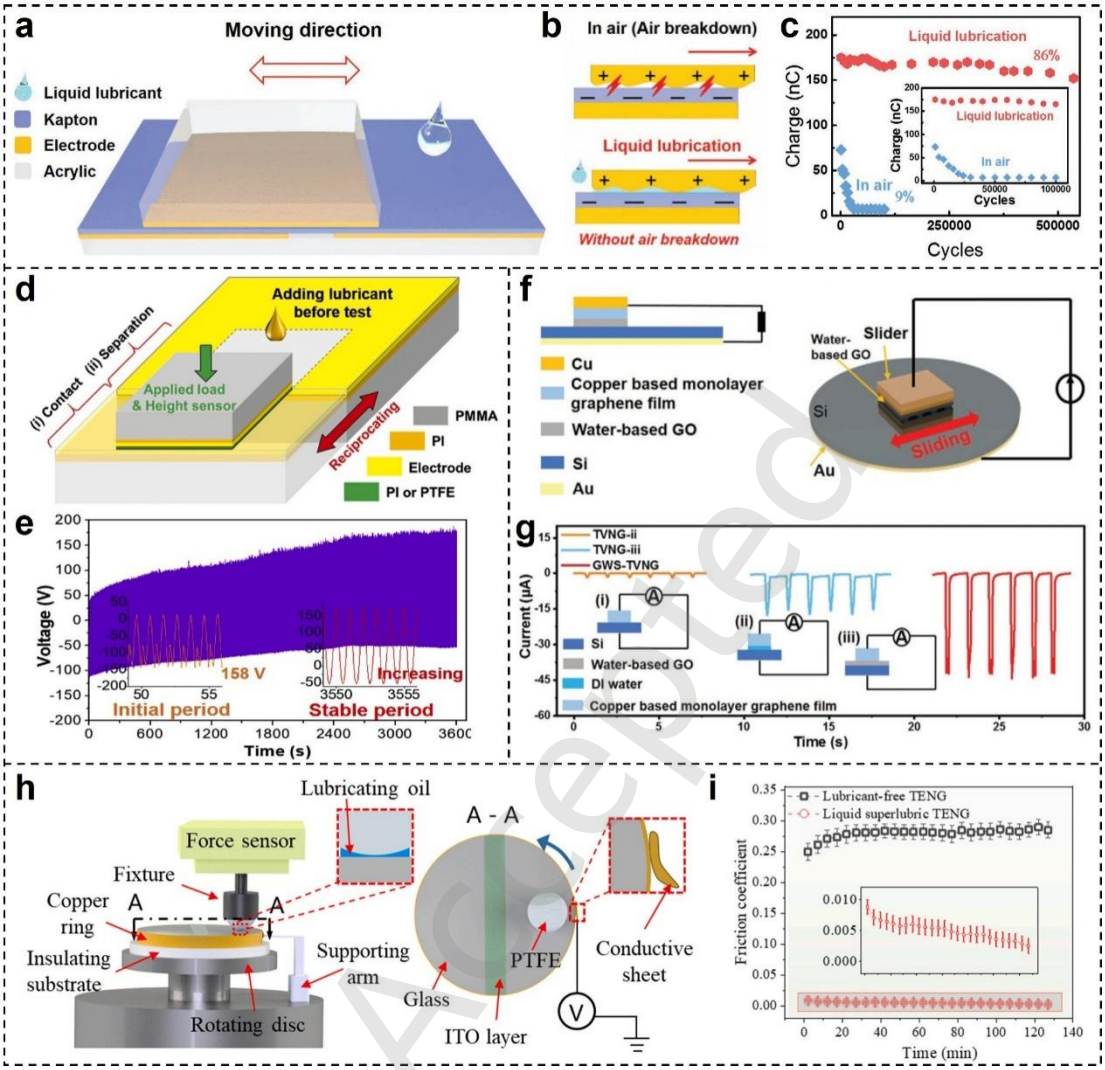

Figure 11. Structural designs based on interface lubrication in TENGs. (a) Structural schematic of sliding freestanding TENG with interface liquid lubrication; (b) Schematic of interfacial breakdown in air and interface liquid lubrication; (c) Durability test of TENG in air and with interface liquid lubrication [86]; (d) Schematic of the slide-mode TENG; (e) Voltage of TENG under squalane-lubricated conditions [87]; (f) Schematic of the TVNG with interface lubrication; (g) Comparison of short circuit current under different interface conditions [88]; (h) Schematic of the liquid superlubric TENG; (i) COF of TENG with and without liquid lubrication [89].

To provide a clearer demonstration of the friction-reduction and anti-wear effects, we have retrieved and compiled relevant literature. Specifically, we have conducted a

quantitative comparison of key characteristic parameters, including cycles for stable output, coefficient of friction before and after lubrication and wear characterization, as shown in Table 1. The results indicate that the introduction of lubrication consistently leads to a substantial reduction in coefficient of friction (CoF) across various material systems and experimental configurations. In most reported cases, the CoF is reduced by one order of magnitude or more, highlighting the remarkable effectiveness of lubrication in suppressing interfacial shear and frictional dissipation. In addition, significant improvements in wear resistance are observed. The reported wear volume, wear depth and wear rate are markedly reduced after lubrication. Moreover, surface morphology analyses consistently reveal smoother wear tracks, reduced transfer film formation and lower surface roughness, further confirming the protective role of lubricating layers in mitigating interfacial damage. It is also worth noting that, beyond friction and wear reduction, lubrication contributes to enhanced operational stability during long-term cycling. Even under high-speed sliding or extended operation durations, lubricated interfaces maintain relatively low CoF and minimal degradation, demonstrating their robustness for practical applications. This quantitative analysis clearly demonstrates that interface lubrication is not only an effective strategy for reducing friction but also plays a critical role in suppressing wear and prolonging device lifespan.

Table1. Comparison of friction reduction and anti-wear effects under interface lubrication strategies

Years	**Cycles for**	**CoF before**	**CoF after**	**Wear characterization**	**Ref.**
2020	60k	0.55	0.04	Wear volume is reduced by about 90%, and	[90]

2021	Slide at 125	0.18	0.04	Wear volume and depth decreased by 96%	[91]
2022	108k	0.22	0.048	Wear of PTFE is greatly reduced, and	[92]
2022	14k	0.4	0.06	Wear marks are shallower and more	[93]
2022	20k	0.76	0.16	Wear loss decreased by 99.5%, wear rate per unit normal load decreased from 0.107	[94]
2023	Slide at 1000	0.26	0.008	Wear rate decreased from 15.70×10^{-5}	[95]
2023	350k	1.403	0.195	Wear of tribo-pair was significantly	[96]
2024	1m	0.8	0.127	Wear depth of polysilicon surface	[97]
2024	60k	Average	/	Friction pair has almost no scratches and	[98]
2024	Almost 180k	0.18	0.1-0.14	Wear loss of PTFE is reduced by 88.5%-	[99]
2024	100k	/	0.077	No obvious wear on the surface and the	[100]
2024	38.1k	0.285	0.0025	Wear rate decreased from 1.07×10^{-3}	[89]
2024	Slide at 80	0.31	0.066	Wear rate of PTFE film reduced to the level	[101]
2025	30k	0.59	0.12	Surface roughness reduced by 2.5 times	[102]
2025	1m	Friction reduced by 72.5 times		The 10-hour continuous operation interface	[103]
2026	21.6m	0.15	0.07	Wear rate decreased by 24.4%	[104]

The structural implementations of interface lubrication establish a foundational strategy to manage friction and wear in TENGs. Based on this, the application of interfacial lubrication in TENGs has attracted extensive attention and research in recent years. Zhang et al. proposed a macro-superlubric TENG that couples structural superlubricity with tribovoltaic DC output [43], enabling simultaneous energy

harvesting and tribological state sensing under high contact stress (Figure 12a-d). The device adopts a ball-on-disc pair of a hydrogenated diamond-like carbon (DLC) film and a steel ball, operating under dry N_2 to maintain a COF < 0.01 while producing unipolar DC output via the tribovoltaic effect. Benefiting from the stable superlubric interface, a peak short circuit current of about 60 nA and a power density up to 5.815 W/m^2 were obtained from the SL-TENG under high contact stress, and it can illuminate multiple LEDs without rectification, enabling intuitive readout of the electrical state. Importantly, switching the atmosphere between N_2 and air induces synchronous variations in COF and current, so the electrical signal can serve as an early-warning indicator of frictional regime transition (Figure 12c–d). An et al. exploited superlubricity interfaces to realize microvalves that are simultaneously airtight, wear-free and intrinsically self-sensing [105], which is a novel application-oriented extension of interface-lubrication concepts into microfluidics. They constructed a superlubricity microvalve by forming a structural superlubricity heterointerface between a valve seat and an HOPG-integrated valve plate, which provides complete sealing for stringent air control (Figure 12e-f). The structural superlubricity interface achieves zero helium leakage at 0.9 MPa and maintains structural integrity after 1 million impact cycles and 5 thousand reciprocating sliding tests (100 μN), as depicted in Figure 12g-h, demonstrating its long-term durability under repetitive actuation. Beyond sealing, a microscale structural superlubricity-TENG is designed as a self-powered displacement transducer. As shown in Figure 12i, the measured voltage–displacement relation matches theoretical predictions, enabling accurate monitoring of valve opening for

closed-loop control without external sensors.

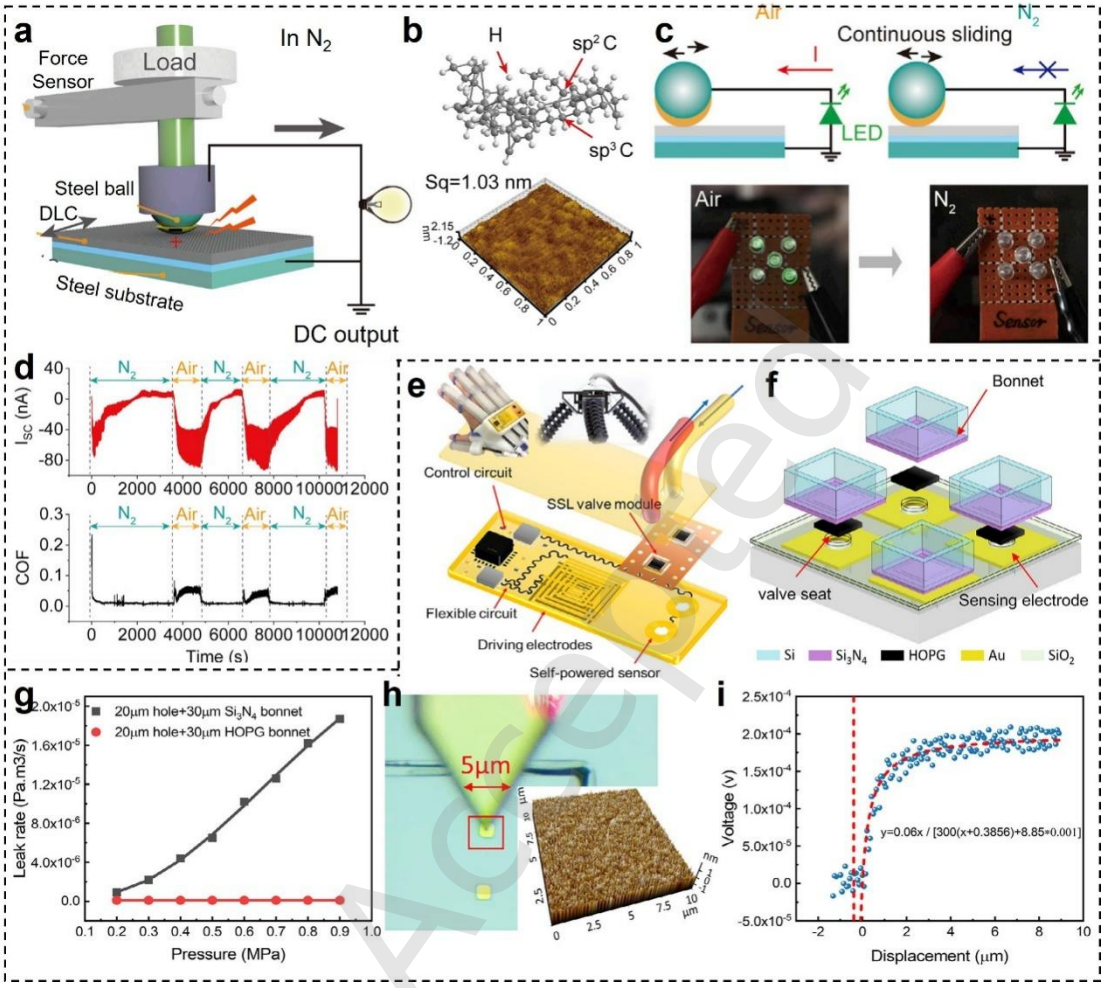

Figure 12. Applications of interface lubrication in TENGs. (a) Schematic of the macro-superlubric TENG; (b) Molecular structure and AFM image of the DLC film; (c-d) Monitoring the failure of superlubric friction and the corresponding changes in Isc and COF [43]; (e-f) Integrated structure of the micro air-driven system and schematic of a superlubricity valve group; (g-h) Sealing performance and sliding cycle durability test; (i) Self-powered real-time monitoring of valve's operational state [105].

7. Comparison of mechanical friction-reduction strategies in TENGs

Building upon the detailed analyses of individual mechanical friction-reduction strategies in the preceding sections, this section provides a systematic and quantitative comparison of the five representative approaches: rolling friction, soft contact,

intermittent contact, non-contact, and interface lubrication. To evaluate their effectiveness in practical applications, these strategies are benchmarked against a unified set of key performance metrics for TENGs, including output retention, operational durability, output power and structural complexity, as shown in Table 2 [41,42,46,49,66,70,71,73,79,80,86,88,102,106–112]. This comparative framework is intended to support rational selection and application-specific optimization of friction-reduction methods in future TENGs designs.

Table 2. Comparison of different mechanical friction-reduction strategies in TENGs

Output retention rate	Output holding value (Q/U/I)	Maximum output power/power density	Output type	Structural complexity	Applicable scenarios	Ref.
98.5	/	280 W/m^2	AC	Moderate	Ambient Energy Harvesting & Monitoring (Wind, Fluid Kinetic); Mechanical Component Energy Harvesting & Condition Monitoring (Bearings, etc.)	[49]
95%	≈11 μA	1.3 mW-100 rpm	AC			[106]
95%	≈3.1 μA	36 μW-0.22 m/s	AC			[107]
98.9	/	3.2 mw-4.5 m/s	AC			[46]
97.24%	≈74 V	28 μW	AC	Simple	Irregular, Low-Frequency Environmental Energy Harvesting and Parameter Monitoring, such as wind energy and wave energy	[66]
99%	≈2.3 μA	/	DC			[108]
93%	≈1.6 V	0.35 μW-2644 rpm	AC			[109]
89.26%	152.06 V	/	AC			[110]
90%	/	/	AC	Medium-high	Energy harvesting devices capable of adapting interface operating modes in response to varying external excitation parameters	[41]
94%	/	19 mW-420 rpm	AC			[71]
90%	/	0.5 mW-3 m/s	AC			[70]
82%	/	0.23 mW-5 m/s	AC			[73]
>100%	≈840 nC	16.7 mW-7m/s	AC	Medium-high	Wind energy or wave energy harvesters intended for long-term operation, always integrated with charge-pumping strategy	[42]
95%	≈105.7 nC	75.96 μW-300 rpm	AC			[79]
≈100%	/	31.3 W/m^3	AC			[80]
99.36%	≈7.8 V	≈13 μW-120 rpm	AC			[111]
86%	152 nC	3.45 W/m^2/Hz	AC & DC	Simple	Energy harvesting and friction interface state monitoring of industrial friction components	[86]
95%	≈30 μA	54.3 mW/m^2	DC			[88]
90%	5.5 V	1.23 mW/m^2	AC			[112]
~99%	≈7.87 μA	2.23 mW/m^2	DC			[102]

In terms of operational durability, non-contact strategies consistently achieve the highest cycle counts (achieving 6.5 million cycles) because they entirely eliminate physical wear by separating friction-pair materials through ingenious structural design. Similarly, rolling friction approach replace sliding with rolling motion, significantly reduce shear forces and abrasive wear, enabling durability in the range of hundreds of thousands to millions of cycles. In contrast, while interface lubrication and soft contact can maintain high output retention (> 90%) within the tested ranges, their typical operational lifespan (tens to hundreds of thousands of cycles) is often limited by the gradual degradation or depletion of the lubricant or the viscoelastic material itself. Regarding output performance, the maximum power density varies significantly influenced by the energy conversion principle and structural design. Notably, several high-power demonstrations in intermittent contact and non-contact strategies (e.g., reaching tens of mW) frequently employ charge pumping or charge excitation strategies. This explains why power outputs within the same strategy category can span orders of magnitude. In addition, the types of TENGs compatible with different friction-reduction strategies vary, which in turn lead to differences in output signal types. Based on the working mechanisms discussed earlier, all five mechanical friction-reduction strategies are applicable to TENGs, which typically generate alternating current (AC) outputs. In contrast, rolling friction and interface lubrication strategies are also compatible with TVNGs, which exhibit direct current (DC) output characteristics. For TENGs employing these two strategies, the nature of the output signal is primarily determined by the tribo-pair material combination. Finally, structural complexity represents a

critical practical trade-off. Soft contact and interface lubrication strategies typically involve minor structural modifications, such as adding a compliant layer or applying a lubricant, thus offering ease of integration and low fabrication barriers. rolling friction introduces moderate complexity due to the incorporation of components like bearings or rotor-stator assemblies. In contrast, intermittent contact and non-contact strategies often entail higher design sophistication, which require precise control over contact-separation timing and gap distances. What's more, achieving higher charge density and overall output performance often necessitates the incorporation of charge pumping architectures.

The above comparative analysis elucidates that no single friction-reduction strategy universally outperforms others across all metrics. Instead, each entails trade-offs rooted in its fundamental working mechanism. These trade-offs span output efficiency, operational durability, structural complexity and output characteristics, forming a multi-dimensional selection space. Collectively, these comparative analysis highlights that the optimal strategy depends on application-specific priorities, such as maximizing service life, achieving high output, minimizing complexity or tailoring the output type, thus offering a rational framework for TENGs design optimization.

8. Conclusions and perspectives

8.1 Summary of mechanical friction-reduction strategies

The five mechanical friction-reduction strategies discussed above (rolling friction, soft contact, intermittent contact, non-contact and interface lubrication) represent different unique design philosophies in TENGs. Rolling friction replaces sliding with

rolling motion to reduce lateral shear and wear. Soft contact relies on compliant materials to buffer contact forces and extend surface longevity. Intermittent contact leverages periodic engagement to minimize cumulative frictional damage. Non-contact systems eliminate material wear through direct physical separation. Finally, interface lubrication techniques aim to minimize frictional force at the molecular level through the introduction of functional surface layers or fluid films. While differing in implementation, these strategies can be qualitatively assessed across several performance dimensions that are critical for TENGs applications. Non-contact strategy excels in wear resistance and long-term durability but generally yields lower energy output and involves higher structural complexity. Rolling friction and soft contact strategies strike a middle ground in output performance, structural complexity and robustness, offering good adaptability to various environments. Intermittent contact achieves high peak power and effective charge accumulation but typically requires more sophisticated mechanical design and precise timing control. Interface lubrication provides moderate output and excellent friction suppression in simple structures, though its long-term reliability can be constrained by lubricant degradation.

These patterns highlight two fundamental trade-offs that constrain TENGs optimization. The one lies in the durability versus output. Non-contact designs offer exceptional mechanical longevity by eliminating wear, but the absence of real contact limits surface charge transfer and thereby reduces power output. Conversely, contact-based strategies such as soft or intermittent contact enable higher energy conversion efficiency but face material degradation due to repetitive interface stress and abrasion.

The second trade-off exists between structural complexity and reliability. Rolling friction or dynamic intermittent contact can achieve superior friction reduction, but they often depend on finely tuned structures. On the other hand, structurally simple approaches like interface lubrication or soft contact are easier to integrate and broadly applicable, yet their performance is frequently constrained by the material properties or long-term stability of lubricants and interfaces. This balance between implementation simplicity and operational reliability is crucial for determining whether a strategy can be widely adopted or remains niche in scope.

8.2 Towards integrated and intelligent TENGs

As TENGs evolve beyond fundamental laboratory prototypes toward multifunctional and practical application systems, the next generation of mechanical friction-reduction strategies must move beyond single function. Current friction-reduction strategies are effective in addressing specific wear-related issues. However, they struggle under the multifactorial and dynamic conditions of practical applications, which involve varying mechanical loads, temperatures, humidity levels, surface contamination and irregular motion patterns. To meet these challenges, future TENGs are expected to adopt integrated and intelligent architectures that enable real-time adaptation of frictional interfaces and energy harvesting performance, including hybridization of multiple strategies, dynamic intelligent interface modulation and multifunctional integrated systems, as depicted in Figure 13.

The hybridization of multiple friction-reduction strategies within a single device represents an effective and potential approach. For instance, combining soft contact

interfaces with intermittent contact mechanisms can not only reduce sustained friction but also enhance conformability under varying mechanical stimuli. Similarly, coupling rolling friction elements with lubricated surfaces may extend operational lifespan while maintaining stable output in cyclic motion scenarios. Such multi-modal approaches require careful material matching, structural synchronization, and mechanical-electrical coupling optimization.

The dynamic modulation of frictional interfaces in response to environmental or mechanical stimuli constitutes a promising path toward intelligent TENGs. This can be achieved by incorporating intelligent responsive materials such as shape memory alloys and stimuli-responsive polymers. These smart materials can adjust contact force or surface texture in real time, thereby enabling TENGs to self-regulate functional interface status under fluctuating conditions. Such intelligent responsiveness provides a foundation for adaptive systems that can maintain optimal output performance without external intervention.

The integration of sensing, feedback, computational modules and friction-reduction architecture enables TENGs to move from passive energy harvesters to active and adaptive triboelectric energy systems. By embedding microsensors and microcontrollers, TENGs can monitor wear status, output fluctuations and then dynamically adjust contact conditions through actuated microstructures, variable-gap designs or surface state modulation. Such intelligent systems could be valuable in applications requiring long-term deployment and autonomous operation, such as structural health monitoring, wearable biosensing and IoT networks.

In this context, the development of intelligent TENGs aligns with emerging trends in self-powered systems, soft robotics and functional materials engineering. The implementation of friction-reduction strategies within such systems must account not only for performance benefits, but also for design scalability, manufacturing compatibility and long-term operational stability. Achieving this balance will require interdisciplinary collaboration across materials science, mechanical design, electronics integration and system-level control.

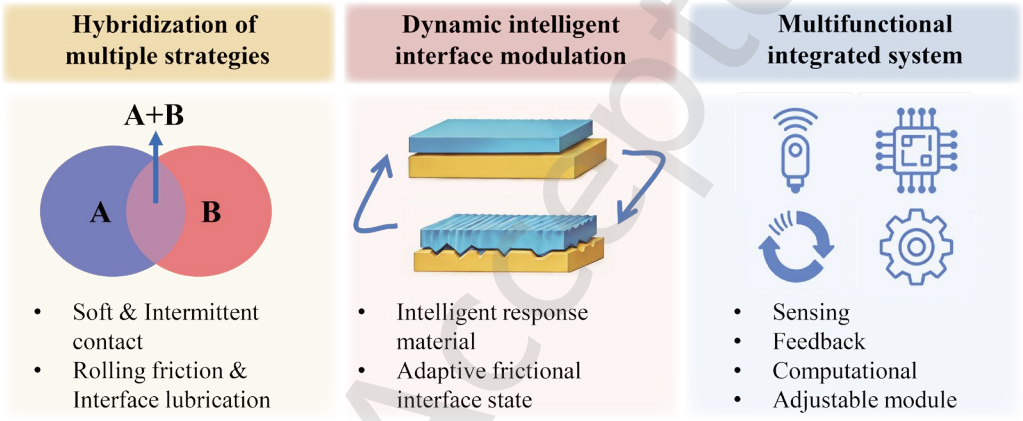

Figure 13. Prospects of mechanical friction-reduction strategies in TENGs.

8.3 Roadmap for commercialization and practical applications

Most reported TENGs demonstrate excellent performance in controlled environments, but their long-term operation in practical settings is constrained by multiple factors including mechanical instability, environmental sensitivity, limited durability and high fabrication complexity. To enable practical deployment, friction-reduction strategies must be re-evaluated from a systems engineering perspective that prioritizes scalability, reliability and manufacturability.

Figure 14 presents the roadmap for the commercialization and practical application of TENGs, primarily encompassing reliability, manufacturability, and

scalability. The materials and structural stability of TENGs over extended operation cycles is a critical barrier to realize commercialization. Friction-reduction strategies that involve soft materials or lubricants may suffer from wear, leakage or interfacial degradation during long-term operation. In addition, ensuring uniform performance across large-area or batch-fabricated devices remains technically difficult, especially for strategies that depend on precise microstructural alignment or controlled surface chemistry. To address these issues, future research needs focus on the development of robust materials, such as wear-resistant composites, stable solid lubricants and self-healing interfaces, that are compatible with industrial-scale manufacturing processes. On the other hand, it is imperative to tailor the TENGs architecture for specific application domains, such as wearable electronics, autonomous sensors, structural health monitoring and low-power embedded systems. Accordingly, application-oriented standardization including testing protocols, durability benchmarks, and performance metrics under realistic scenarios will be essential for building TENGs-based energy solutions. What's more, developing integrated energy management systems that combine TENGs with power management circuits, energy storage modules and wireless transmission units is necessary.

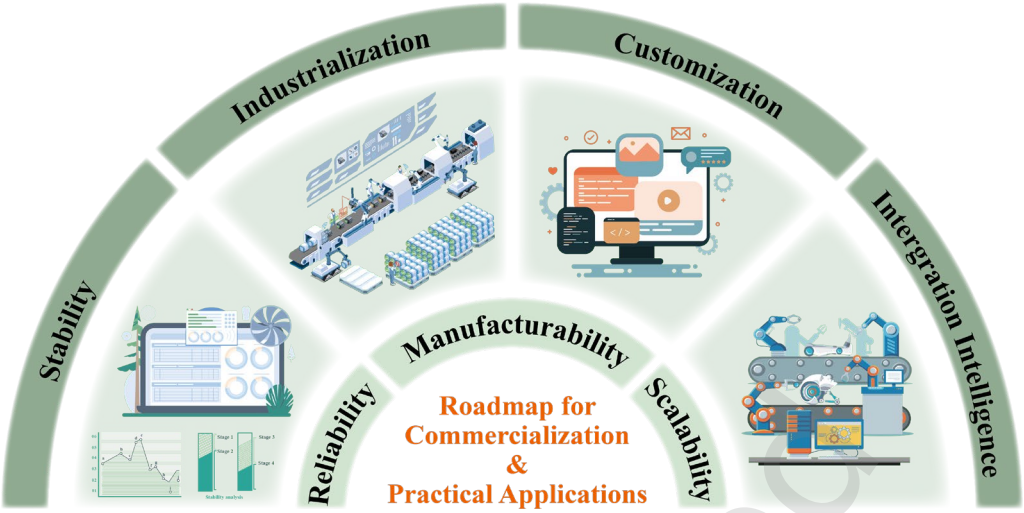

Figure 14. Roadmap for commercialization and practical applications of TENGs.

Ultimately, the commercialization of TENGs depends not only on improving individual device performance, but also on creating holistic, scalable and application platforms. By aligning materials research, device engineering and systems integration, friction-optimized TENGs are poised to become a foundational component of the next generation of sustainable, distributed and self-powered technologies.

Acknowledgements

This work is supported by the National Natural Science Foundation of China (52505188, 52275191, 52450006), Postdoctoral Fellowship Program of CPSF (GZC20250899), Jiangsu Funding Program for Excellent Postdoctoral Talent (2025ZB830).

Conflict of Interest

The authors declare that they have no conflicts of interest in this work.

Reference

[1] Chen X, Lu C, Liu X, Sun T, Mo J. The Influence of Competition between Thermal Expansion and Braking Parameter on the Wear Degradation of Friction Block.

Tribol. Int. 192, 109246, 2024.

[2] Wang P, Feng Y, Wu Z, Liu C, Sun W, Wang D. In-Situ Monitoring and Wear Warning of MAO-al/Resin Coatings by Interface Triboelectrification. J. Alloys Compd. 1020, 179577, 2025.

[3] Lei Y, Feng Y, Wu Z, Gao Q, Zhang Z, Wang W, Wang L, Wang Y, Wang D. Monitoring of Lubrication and Wear in-Situ by Triboelectrification under Grease Lubrication. Friction 13 (2), 9440938, 2025.

[4] Qi Y, Zhao J, Zeng J, Cao X, Qin Y, Cao J, Gong L, Huang X, Wang Z, Liu G, Zhang C. Self-Powered Wireless Temperature and Vibration Monitoring System by Weak Vibrational Energy for Industrial Internet of Things. ACS Applied Materials & Interfaces 2023.

[5] Wen D-L, Huang P, Deng H-T, Zhang X-R, Wang Y-L, Zhang X-S. High-Performance Hybrid Nanogenerator for Self-Powered Wireless Multi-Sensing Microsystems. Microsyst Nanoeng 9 (1), 94, 2023.

[6] Huang L, Huang G, Zhang D, Chen X. Diversified Applications of Triboelectric and Electrostatic Effect. Friction 13 (2), 9440893, 2025.

[7] Deng W, Dong K, Ni S, He S, Zhao P, Yu T, Zhao J. Magnet Gear-Based Triboelectric Nanogenerator Harvesting Energy from Boiling Heat Transfer Environment. NANO ENERGY 137, 2025.

[8] Tao X, Wang T, Tan L, Xu F, Chen A, Yang Y, Zhang R, Wang X. High-Performance Constant Current Triboelectric Nanogenerator for Wind Energy Harvesting and Air Purification. SmartSys 1 (4), e70012, 2025.

[9] Wu B, Zhang Z, Xue X, Hao C, Zhang W, Bi R, Wang Q, Xue C. A Stretchable Triboelectric Generator with Coplanar Integration Design of Energy Harvesting and Strain Sensing. Science China-Technological Sciences 65 (1), 221–230, 2022.

[10] Tian J, Wang F, Ding Y, Lei R, Shi Y, Tao X, Li S, Yang Y, Chen X. Self-Powered Room-Temperature Ethanol Sensor Based on Brush-Shaped Triboelectric Nanogenerator. Research 2021, 2021.

[11] Zhang Z, Wu N, Gong L, Luan R, Cao J, Zhang C. An Ultrahigh Power Density and Ultralow Wear GaN-Based Tribovoltaic Nanogenerator for Sliding Ball Bearing as Self-Powered Wireless Sensor Node. Advanced Materials 36 (6), 2024.

[12] Cao J, Dong Z, Zhang Z, Gong L, Gao Y, Dai Y, Liu G, Feng Y, Jin Z, Luan R, Wang Z, Dong S, Cheng G, Zhang C, Ding J. A Power-Managed Tribovoltaic Nanogenerator and Self-Powered Wireless Temperature Monitoring System. Advanced Energy Materials 14 (22), 2024.

[13] Zhou L, Liu D, Wang J, Wang Z L. Triboelectric Nanogenerators: Fundamental Physics and Potential Applications. Friction 8 (3), 481–506, 2020.

[14] Wu C, Wang A C, Ding W, Guo H, Wang Z L. Triboelectric Nanogenerator: A Foundation of the Energy for the New Era. Advanced Energy Materials 9 (1), 1802906, 2019.

[15] Qin Y, Fu X, Lin Y, Wang Z, Cao J, Zhang C. Self-Powered Internet of Things Sensing Node Based on Triboelectric Nanogenerator for Sustainable Environmental Monitoring. Nano Research 16 (9), 11878–11884, 2023.

[16] Zhang Z, Jiang D, Zhao J, Liu G, Bu T, Zhang C, Wang Z L. Tribovoltaic Effect

on Metal–Semiconductor Interface for Direct-Current Low-Impedance Triboelectric Nanogenerators. Advanced Energy Materials 10 (9), 1903713, 2020.

[17] Chen J, Wang Z L. Reviving Vibration Energy Harvesting and Self-Powered Sensing by a Triboelectric Nanogenerator. Joule 1 (3), 480–521, 2017.

[18] Xing F, Gao X, Gao W, Sun Y, Zhao Z, Wang Z L, Chen B. High-Entropy Energy for Self-Powered Systems. SmartSys 1 (2), e70001, 2025.

[19] Wang Z L, Wang A C. On the Origin of Contact-Electrification. Materials Today 30, 34–51, 2019.

[20] Dong B, Shi Q, Yang Y, Wen F, Zhang Z, Lee C. Technology Evolution from Self-Powered Sensors to AIoT Enabled Smart Homes. Nano Energy 79, 105414, 2021.

[21] Pu X, Wang Z L. Self-Charging Power System for Distributed Energy: Beyond the Energy Storage Unit. Chem. Sci. 12 (1), 34–49, 2021.

[22] Jiang Z, Dong Z, Fu X, Gao Z, Gong L, Cao J, Qi Y, Liu T, Li W, Zhang C. Weak Vibration Energy Powered Acceleration Monitoring System for Bearing Fault Diagnosis. Mechanical Systems and Signal Processing 244, 113823, 2026.

[23] Cao J, Lin Y, Fu X, Wang Z, Liu G, Zhang Z, Qin Y, Zhou H, Dong S, Cheng G, Zhang C, Ding J. Self-Powered Overspeed Wake-up Alarm System Based on Triboelectric Nanogenerators for Intelligent Transportation. Nano Energy 107, 108150, 2023.

[24] Zhu Q, Zhu L, Wang Z, Zhang X, Li Q, Han Q, Yang Z, Qin Z. Hybrid Triboelectric-Piezoelectric Nanogenerator Assisted Intelligent Condition Monitoring for Aero-Engine Pipeline System. Chem. Eng. J. 519, 165121, 2025.

[25] Gu W, Cao J, Dai S, Hu H, Zhong Y, Cheng G, Zhang Z, Ding J. Self-Powered Slide Tactile Sensor with Wheel-Belt Structures Based on Triboelectric Effect and Electrostatic Induction. Sens. Actuators, A 331, 113022, 2021.

[26] Liu H, Cao J, Feng S, Cheng G, Zhang Z, Ding J. Highly Sensitive and Durable, Triboelectric Based Self-powered Nanosensor for Boundary Detection in Sports Event. Advanced Materials Technologies 8 (8), 2201766, 2023.

[27] Wang Z, Liu G, Cao J, Fu X, Fan B, Qin Y, Wang Z, Zhang Z, Chen Y, Zhang C. Self-powered Position Monitoring System Based on Insole-type Wearable Triboelectric Nanogenerator and Bluetooth Beacon. Adv. Mater. Technol. 8 (18), 2300487, 2023.

[28] Xu C, Yu J, Huo Z, Wang Y, Sun Q, Wang Z L. Pursuing the Tribovoltaic Effect for Direct-Current Triboelectric Nanogenerators. Energy & Environmental Science 16, 983–1006, 2023.

[29] Zhang Z, Gong L, Luan R, Feng Y, Cao J, Zhang C. Tribovoltaic Effect: Origin, Interface, Characteristic, Mechanism & Application. Advanced Science 11 (15), 2305460, 2024.

[30] Liu J, Goswami A, Jiang K, Khan F, Kim S, McGee R, Li Z, Hu Z, Lee J, Thundat T. Direct-Current Triboelectricity Generation by a Sliding Schottky Nanocontact on MoS2 Multilayers. Nature Nanotechnology 13 (2), 112–116, 2018.

[31] Liu J, Miao M, Jiang K, Khan F, Goswami A, McGee R, Li Z, Nguyen L, Hu Z, Lee J, Cadien K, Thundat T. Sustained Electron Tunneling at Unbiased Metal-Insulator-Semiconductor Triboelectric Contacts. Nano Energy 48, 320–326, 2018.

[32] Lin S, Lu Y, Feng S, Hao Z, Yan Y. A High Current Density Direct-Current Generator Based on a Moving van Der Waals Schottky Diode. Advanced Materials 31 (7), 1804398, 2018.

[33] Chen Y, Zhang Z, Wang Z, Bu T, Dong S, Wei W, Chen Z, Lin Y, Lv Y, Zhou H, Sun W, Zhang C. Friction-Dominated Carrier Excitation and Transport Mechanism for GaN-Based Direct-Current Triboelectric Nanogenerators. ACS Appl. Mater. Interfaces 14 (20), 24020–24027, 2022.

[34] Zhao W, Liu L, Shang Y, Wang X, Han R, Chen P, Wang Z L, Jiang T. High-Durability in-Phase-Stacked Triboelectric Nanogenerators with Dual-Roller Charge Enhancement for Ocean Energy Harvesting. Advanced Energy Materials DOI: 10.1002/aenm.70891, online, 2026.

[35] Wang S, Xie Y, Niu S, Lin L, Wang Z L. Freestanding Triboelectric-Layer-Based Nanogenerators for Harvesting Energy from a Moving Object or Human Motion in Contact and Non-contact Modes. Advanced Materials 26 (18), 2818–2824, 2014.

[36] Lin L, Xie Y, Niu S, Wang S, Yang P-K, Wang Z L. Robust Triboelectric Nanogenerator Based on Rolling Electrification and Electrostatic Induction at an Instantaneous Energy Conversion Efficiency of ~55%. ACS Nano 9 (1), 922–930, 2015.

[37] Li X H, Han C B, Jiang T, Zhang C, Wang Z L. A Ball-Bearing Structured Triboelectric Nanogenerator for Nondestructive Damage and Rotating Speed Measurement. Nanotechnology 27 (8), 085401, 2016.

[38] Zhang B, Zhang L, Deng W, Jin L, Chun F, Pan H, Gu B, Zhang H, Lv Z, Yang W, Wang Z L. Self-Powered Acceleration Sensor Based on Liquid Metal Triboelectric Nanogenerator for Vibration Monitoring. ACS Nano 11 (7), 7440–7446, 2017.

[39] Zhang S L, Xu M, Zhang C, Wang Y-C, Zou H, He X, Wang Z, Wang Z L. Rationally Designed Sea Snake Structure Based Triboelectric Nanogenerators for Effectively and Efficiently Harvesting Ocean Wave Energy with Minimized Water Screening Effect. Nano Energy 48, 421–429, 2018.

[40] Lin Z, Zhang B, Guo H, Wu Z, Zou H, Yang J, Wang Z L. Super-Robust and Frequency-Multiplied Triboelectric Nanogenerator for Efficient Harvesting Water and Wind Energy. Nano Energy 64, 103908, 2019.

[41] Chen J, Guo H, Hu C, Wang Z L. Robust Triboelectric Nanogenerator Achieved by Centrifugal Force Induced Automatic Working Mode Transition. Advanced Energy Materials 10 (23), 2000886, 2020.

[42] Long L, Liu W, Wang Z, He W, Li G, Tang Q, Guo H, Pu X, Liu Y, Hu C. High Performance Floating Self-Excited Sliding Triboelectric Nanogenerator for Micro Mechanical Energy Harvesting. Nat Commun 12 (1), 4689, 2021.

[43] Zhang L, Cai H, Xu L, Ji L, Wang D, Zheng Y, Feng Y, Sui X, Guo Y, Guo W, Zhou F, Liu W, Wang Z. Macro-Superlubric Triboelectric Nanogenerator Based on Tribovoltaic Effect. Matter 5 (5), 2022.

[44] He L, Zhang C, Zhang B, Gao Y, Yuan W, Li X, Zhou L, Zhao Z, Wang Z, Wang J. A High-Output Silk-Based Triboelectric Nanogenerator with Durability and

Humidity Resistance. Nano Energy 108, 2023.

[45] Bu T, Deng W, Liu Y, Wang Z L, Chen X, Zhang C. Submillimeter-Scale Superlubric Triboelectric Nanogenerator. Adv Funct Materials 34 (40), 2404007, 2024.

[46] Zhu J, Fan K, Wang W, Zhai K, Zhang L, Zhou J, Li C, Li Y, Li J, Liu Y, Ren Z, Wang P. A Robust Hybrid Nanogenerator Strategy Achieved by Regenerative Motion Transmission toward Wind Energy Harvesting and Self-Powered Sensing. Nano Energy 135, 110679, 2025.

[47] Fu X, Pan X, Liu Y, Li J, Zhang Z, Liu H, Gao M. Non-Contact Triboelectric Nanogenerator. Advanced Functional Materials 33 (52), 2306749, 2023.

[48] Fu S, Hu C. Achieving Ultra-Durability and High Output Performance of Triboelectric Nanogenerators. Advanced Functional Materials 34 (9), 2308138, 2024.

[49] Tang Q, Wang Z, Chang W, Sun J, He W, Zeng Q, Guo H, Hu C. Interface Static Friction Enabled Ultra-Durable and High Output Sliding Mode Triboelectric Nanogenerator. Adv Funct Materials 32 (26), 2202055, 2022.

[50] Fu X, Xu S, Gao Y, Zhang X, Liu G, Zhou H, Lv Y, Zhang C, Wang Z. Breeze-Wind-Energy-Powered Autonomous Wireless Anemometer Based on Rolling Contact-Electrification. ACS Energy Letters 6 (6), 2343–2350, 2021.

[51] Yuan H, Xiao Z, Wan J, Xiang Y, Dai G, Li H, Yang J. A Rolling-Mode Al/CsPbBr3 Schottky Junction Direct-Current Triboelectric Nanogenerator for Harvesting Mechanical and Solar Energy. Advanced Energy Materials 12 (25),

2200550, 2022.

[52] Dong F, Zhu M, Wang Y, Chen Z, Dai Y, Xi Z, Du T, Xu M. AI-Enabled Rolling Triboelectric Nanogenerator for Bearing Wear Diagnosis Aiming at Digital Twin Application. Nano Energy 134, 110550, 2025.

[53] Xi Z, Du H, Wang Y, Yu H, Dai S, Fan M, Liu J, Su Q, Wang H, Hu G, Xu M. A Ternary-Dielectric Rolling TENG Array for Robust Ocean Energy Harvesting and Distributed Environmental Monitoring. Nano Energy 143, 111318, 2025.

[54] Dong S, Bu T, Wang Z, Feng Y, Liu G, Zeng J, Wang Z, Cao J, Zhang Z, Liu F, Zhang C. Freestanding-Mode Tribovoltaic Nanogenerator for Harvesting Sliding and Rotational Mechanical Energy. Advanced Energy Materials 13 (16), 2300079, 2023.

[55] Wu R, Liu S, Lin Z, Zhu S, Ma L, Wang Z. Industrial Fabrication of 3D Braided Stretchable Hierarchical Interlocked Fancy-Yarn Triboelectric Nanogenerator for Self-Powered Smart Fitness System. Advanced Energy Materials 12 (31), 2022.

[56] Xie Z, Wang Y, Wu R, Yin J, Yu D, Liu J, Cheng T. A High-Speed and Long-Life Triboelectric Sensor with Charge Supplement for Monitoring the Speed and Skidding of Rolling Bearing. Nano Energy 92, 106747, 2022.

[57] Zhang C, Liu Y, Zhang B, Yang O, Yuan W, He L, Wei X, Wang J, Wang Z L. Harvesting Wind Energy by a Triboelectric Nanogenerator for an Intelligent High-Speed Train System. ACS Energy Letters 1490–1499, 2021.

[58] Gao S, Zhang R, Wu F, Luo J, Pu H, Chu F, Han Q. Rotating Single-Electrode Triboelectric V-Belts with Skidding and Wear Monitoring Capabilities. Tribology

International 193, 109404, 2024.

[59] Wang S, Gong L, Jiang Y, Gao S, Wang T, Zhang C, Han Q. Compound Motion-Mode Tribovoltaic Nanogenerator for Self-Powered Monitoring of Gear Transmission System. Advanced Materials Technologies 10 (9), 2025.

[60] Gong L, Zhang Z, Luan R, Feng Y, Gao M, Zhang C. Self-Powered Technologies for Smart Bearings. Fundamental Research 2025.

[61] Han J, Feng Y, Chen P, Liang X, Pang H, Jiang T, Wang Z L. Wind-Driven Soft-Contact Rotary Triboelectric Nanogenerator Based on Rabbit Fur with High Performance and Durability for Smart Farming. Adv Funct Materials 32 (2), 2108580, 2022.

[62] Li X, Cao Y, Yu X, Xu Y, Yang Y, Liu S, Cheng T, Wang Z L. Breeze-Driven Triboelectric Nanogenerator for Wind Energy Harvesting and Application in Smart Agriculture. Applied Energy 306, 117977, 2022.

[63] Pei H, Yang X, Dang Z, Lin W, Li Y, Han S, Cui Y, Bai S, Han W, Cheng L. High Performance Rotary Triboelectric Nanogenerator in Weak Wind Conditions through Soft Contact Utilization. ACS Appl. Electron. Mater. 6 (9), 6802–6809, 2024.

[64] Zhao B, Long Y, Huang T, Niu J, Liu Y, Sha W, Wang J, Wang Z L, Zhai J, Hu W. Self-Adaptive and Soft-Contact Ellipsoidal Pendulum-Structured Triboelectric Nanogenerator for Harvesting Water Wave Energy. Chemical Engineering Journal 489, 151399, 2024.

[65] Liu W, Wang X, Wang Y, Xu H, Nan Y, Niu J, Xiong J, Yang H, Liu T, Yang L.

Enhancing the Output Performance of Triboelectric Nanogenerator Based on Soft-Contact Coaxial Double-Rotation Structure. Advanced Sustainable Systems 8 (4), 2300430, 2024.

[66] Lin Z, Zhang B, Xie Y, Wu Z, Yang J, Wang Z L. Elastic-Connection and Soft-Contact Triboelectric Nanogenerator with Superior Durability and Efficiency. Adv Funct Materials 31 (40), 2105237, 2021.

[67] Yang F, Wang Z, Xu B, Lu Y, Hou X, Xu J, Xie Z. A Soft-Soft Contact Triboelectric Nanogenerator with a Ternary Four-Phase Structure for Self-Powered High-Efficiency Dust Removal on Mars. Advanced Science 12 (27), 2502956, 2025.

[68] Cao H, Ru Q, Fang D, Li S, Liu N, Jiang W, Hu H, Yang Y, Gu G, Zhang B, Cheng G, Yang S, Pang S, Du Z. A Freestanding Rotating Triboelectric Nanogenerator with Large Area and High Efficiency for Triboelectric Plasma CO_2 Reduction. Chemical Engineering Journal 489, 150798, 2024.

[69] Lin Z, Zhang B, Zou H, Wu Z, Guo H, Zhang Y, Yang J, Wang Z L. Rationally Designed Rotation Triboelectric Nanogenerators with Much Extended Lifetime and Durability. Nano Energy 68, 104378, 2020.

[70] Luo Y, Chen P, Cao L N Y, Xu Z, Wu Y, He G, Jiang T, Wang Z L. Durability Improvement of Breeze-Driven Triboelectric-Electromagnetic Hybrid Nanogenerator by a Travel-Controlled Approach. Adv Funct Materials 32 (39), 2205710, 2022.

[71] Fu S, He W, Tang Q, Wang Z, Liu W, Li Q, Shan C, Long L, Hu C, Liu H. An

Ultrarobust and High-Performance Rotational Hydrodynamic Triboelectric Nanogenerator Enabled by Automatic Mode Switching and Charge Excitation. Advanced Materials 34 (2), 2105882, 2022.

[72] Liu Y, Yan W, Han J, Chen B, Wang Z L. Aerodynamics-Based Triboelectric Nanogenerator for Enhancing Multi-Operating Robustness via Mode Automatic Switching. Adv Funct Materials 32 (27), 2202964, 2022.

[73] Fan K, Chen C, Zhang B, Li X, Wang Z, Cheng T, Lin Wang Z. Robust Triboelectric-Electromagnetic Hybrid Nanogenerator with Maglev-Enabled Automatic Mode Transition for Exploiting Breeze Energy. Applied Energy 328, 120218, 2022.

[74] Jin Z, Cao J, Lei R, You J, Mi L, Ju G, Gao Y, Qu Z, Cheng G. Highly Durable Triboelectric Nanogenerator Based on the Chute-Rotating Shaft Intermittent Contact Structure. Acta Phys. Sin. 75 (6), 2026.

[75] Cao J, Fu X, Zhu H, Qu Z, Qi Y, Zhang Z, Zhang Z, Cheng G, Zhang C, Ding J. Self-powered Non-contact Motion Vector Sensor for Multifunctional Human–Machine Interface. Small Methods 6 (8), 2200588, 2022.

[76] Zhang N, Qin C, Feng T, Li J, Yang Z, Sun X, Liang E, Mao Y, Wang X. Non-Contact Cylindrical Rotating Triboelectric Nanogenerator for Harvesting Kinetic Energy from Hydraulics. Nano Res. 13 (7), 1903–1907, 2020.

[77] Lei R, Li S, Shi Y, Yang P, Tao X, Zhai H, Wang Z L, Chen X. Largely Enhanced Output of the Non-Contact Mode Triboelectric Nanogenerator via a Charge Excitation Based on a High Insulation Strategy. Advanced Energy Materials 12

(40), 2201708, 2022.

[78] Hu Y, Li X, Gao Y, Zhao Z, Zhang B, Zhang C, He L, Liu J, Zhou L, Wang Z L, Wang J. A Noncontact Constant-Voltage Triboelectric Nanogenerator via Charge Excitation. ACS Energy Lett. 8 (5), 2066–2076, 2023.

[79] Fu X, Qin Y, Zhang Z, Liu G, Cao J, Fan B, Wang Z, Wang Z, Zhang C. Ultra-Robust and High-Performance Rotational Triboelectric Nanogenerator by Bearing Charge Pumping. Energy & Environmental Materials 7 (2), 2024.

[80] Chen F, Dai X, Wu X, Ding Z, Gao Y, Pang Y, Jiang T, Luo J, Hong Z, Wang Z L. High Energy Density Non-Contact Bidirectional Spinning Oscillating Float-Type Triboelectric Nanogenerators for Energy Extraction From Irregular Waves. Advanced Energy Materials 15 (17), 2404891, 2025.

[81] Ying F, Yu X, Cao J, Li P, Yang L, Guo Y. Real-Time Detection of Rotor Misalignment Using a Non-Contact Triboelectric Sensor Integrated with Deep Learning. Measurement 257, 118704, 2026.

[82] Huang X, Lin L, Zheng Q. Theoretical Study of Superlubric Nanogenerators with Superb Performances. Nano Energy 70, 104494, 2020.

[83] He W, Liu W, Fu S, Wu H, Shan C, Wang Z, Xi Y, Wang X, Guo H, Liu H, Hu C. Ultrahigh Performance Triboelectric Nanogenerator Enabled by Charge Transmission in Interfacial Lubrication and Potential Decentralization Design. Research 2022, 2022.

[84] Wang K, Wu C, Zhang H, Li J, Li J. Cylindrical Bearing Inspired Oil Enhanced Rolling Friction Based Nanogenerator. Nano Energy 99, 2022.

[85] Wang Z, Gao K, Feng Y, Cao J, Gong L, Fan B, Zhang Y, Xie G, Zhang C. Characterizing Superlubricity by Tribovoltaic Effect. Science Bulletin 69 (9), 1197–1201, 2024.

[86] Zhou L, Liu D, Zhao Z, Li S, Liu Y, Liu L, Gao Y, Wang Z L, Wang J. Simultaneously Enhancing Power Density and Durability of Sliding-Mode Triboelectric Nanogenerator via Interface Liquid Lubrication. Advanced Energy Materials 10 (45), 2002920, 2020.

[87] Wu J, Xi Y, Shi Y. Toward Wear-Resistive, Highly Durable and High Performance Triboelectric Nanogenerator through Interface Liquid Lubrication. Nano Energy 72, 2020.

[88] Qiao W, Zhao Z, Zhou L, Liu D, Li S, Yang P, Li X, Liu J, Wang J, Wang Z L. Simultaneously Enhancing Direct-Current Density and Lifetime of Tribovotaic Nanogenerator via Interface Lubrication. Adv Funct Materials 2208544, 2022.

[89] Wang K, Wang X, Sun Y, Wu Z, Zhang H, Xiao K, Du J, Li J, Luo J. Macroscopic Liquid Superlubric Triboelectric Nanogenerator: An in-Depth Understanding of Solid-Liquid Interfacial Charge Behavior. Nano Energy 129, 110038, 2024.

[90] Zhang J, Zheng Y, Xu L, Wang D. Oleic-acid enhanced triboelectric nanogenerator with high output performance and wear resistance. Nano Energy 69, 104435, 2020.

[91] Wang K, Li J, Li J, Wu C, Yi S, Liu Y, Luo J. Hexadecane-containing sandwich structure based triboelectric nanogenerator with remarkable performance enhancement. Nano Energy 87, 106198, 2021.

[92] Guo Y, Zhang L, Du C, Feng Y, Yang D, Zhang Z, Feng M, Wan Y, Wang D. Onion-like carbon as nano-additive for tribological nanogenerators with enhanced output performance and stability. Nano Energy 104, 107900, 2022.

[93] Liu X, Zhang J, Zhang L,Feng Y, Feng M, Luo N, Wang D. Influence of interface liquid lubrication on triboelectrification of point contact friction pair. Tribology International 165, 107323, 2022.

[94] Yang D, Zhang L, Luo N, Liu Y, Sun W, Peng J, Feng M, Feng Y, Wang H, Wang D. Tribological-behaviour-controlled direct-current triboelectric nanogenerator based on the tribovoltaic effect under high contact pressure. Nano Energy 99, 107370, 2022.

[95] Chen J, Zhao Y, Wang R, Wang P. Super-Low Friction Electrification Achieved on Polytetrafluoroethylene Films-Based Triboelectric Nanogenerators Lubricated by Graphene-Doped Silicone Oil. Micromachines 14(9), 1776, 2023.

[96] Zhang X, Liu M, Zhang Z, Min H, Wang C, Hu G, Yang T, Luo S, Yu B, Huang T, Zhu M, Yu H. Highly Durable Bidirectional Rotary Triboelectric Nanogenerator with a Self-Lubricating Texture and Self-Adapting Contact Synergy for Wearable Applications. Small 19(39), 2300890, 2023.

[97] Gong L K, Zhang Z, Yu W B, Zeng J H, Cao J, Fan B B, Zhao J Q, Zhang C. Ultra-Durable Polysilicon Based Tribovoltaic Nanogenerators for Bearing In Situ Rotational Speed Sensing. Small 20 (50), 2405992, 2024.

[98] Chen A, Zeng Q, Tan L, Wang T, Xu F, Wang J, Tao X, Yang Y, Wang X. Charge Accumulation Effect Enabled by a Bioinspired Self-lubricating Triboelectric

Nanogenerator for Both High Average Power Density and Long Durability. Advanced Functional Materials 34(45), 2405698, 2024.

[99] Zhao Z, Wang X, Hu Y, Li Z, Li L, Ye G. Investigation on the tribological properties and electrification performance of grease-lubricated triboelectric nanogenerators. Tribology International 191, 109163, 2024.

[100] Liu M, Zhang X, Xin Y, Guo D, Hu G, Ma Y, Yu B, Huang T, Ji C, Zhu M, Yu H. Earthworm-Inspired Ultra-Durable Sliding Triboelectric Nanogenerator with Bionic Self-Replenishing Lubricating Property for Wind Energy Harvesting and Self-Powered Intelligent Sports Monitoring. Advanced Science 11(28), 2401636, 2024.

[101] Shao J, Yu G, He Y, Li J, Hou M, Wang X, Zhang P, Wang X. An Investigation of the Output Performances of a Triboelectric Nanogenerator Lubricated with TiO2-Doped Oleic Acid. Lubricants 12(8), 269, 2024.

[102] Yuan J, Song W, Le K, Zheng L, Liu Y, Luo Y, Xu S. Boosting Energy Conversion Efficiency in Tribovoltaic Nanogenerators through Graphene-Enhanced Interfacial Lubrication. Chemical Engineering Journal 525, 170088, 2025.

[103] Zhao Y, Feng Y, Gao Q, Li H, Guo X, Wang J, Wang X, Dong L, Yu Y, Wang Z L, Cheng T, Boosting Output Performance of Triboelectric Nanogenerator via Interface Self-Regulation Strategy. Research 8, 0906, 2025.

[104] Zhao K, Zhou J, Zhang C, Qian W, Wu J, Liu Y, Qiang L,Zhong M, Meng C, Wang Y, Zhang K. Layer-Engineered Hybrid MoS_2 Nanosheets for Synergistic Charge Trapping and Superlubrication toward High-Output Ultra-Durable

Triboelectric Nanogenerators. Advanced Functional Materials 36(28), e24763, 2026.

[105] An J, Jiang Y, Jiang T, Li F, Xiang X, Wang K, Tan Z, Nie J, Ren Z. Achieving Zero Leakage, Ultralong Lifespan, and Intrinsic Opening Sensing in Microvalves Through Structural Superlubrication and Triboelectric Nanogenerator Technologies. Advanced Materials 37 (16), 2416132, 2025.

[106] Fu S, He W, Wu H, Shan C, Du Y, Li G, Wang P, Guo H, Chen J, Hu C. High Output Performance and Ultra-Durable DC Output for Triboelectric Nanogenerator Inspired by Primary Cell. Nano-Micro Lett. 14 (1), 155, 2022.

[107] Zhao J, Wang D, Zhang F, Pan J, Claesson P, Larsson R, Shi Y. Self-Powered, Long-Durable, and Highly Selective Oil–Solid Triboelectric Nanogenerator for Energy Harvesting and Intelligent Monitoring. Nano-Micro Lett. 14 (1), 160, 2022.

[108] Guan X, Yao Y, Wang K, Liu Y, Pan Z, Wang Z, Yu Y, Li T. Wireless Online Rotation Monitoring System for UAV Motors Based on a Soft-Contact Triboelectric Nanogenerator. ACS Appl. Mater. Interfaces 16 (35), 46516–46526, 2024.

[109] Wang X, Chen L, Xu Z, Chen P, Ye C, Chen B, Jiang T, Hong Z, Wang Z L. High-Durability Stacked Disc-Type Rolling Triboelectric Nanogenerators for Environmental Monitoring Around Charging Buoys of Unmanned Ships. Small 20 (23), 2310809, 2024.

[110] Shen J, Yang Z, Yang Y, Yang B, Song Y, Cheng X, Lai Z, Zhao H, Ji L, Zhu Z,

Cheng J. A Remote Monitoring System for Wind Speed and Direction Based on Non-Contact Triboelectric Nanogenerator. Nano Energy 133, 110453, 2025.

[111]Zhang J, Li H, Wang J, He S, Wang X, Yu Y, Zhu J, Cheng X, Jiang L, Wang Z L, Cheng T. A Flexible Rolling Triboelectric Nanogenerator with a Bionic Gill Cover Structure for Low-Velocity Water Flow Energy Harvesting. Small 21 (6), 2409864, 2025.

[112] Qian H, Zhang Y, Lu S, Jia X, Long W. Electrification Mechanism and Critical Performance Factors of Animal Fur Fiber-Based Soft-Contact Triboelectric Nanogenerators. Advanced Functional Materials 36 (4), e07688, 2026.

Dr. Jie Cao received his Ph.D. from Jiangsu University in 2024. Now he is doing postdoctoral at Jiangsu University, and as a visiting scholar in Beijing Institute of Nanoenergy and Nanosystems, Chinese Academic Science. His research interests focus on micro-nano energy harvesting, triboelectric transistor and self-powered sensors/systems.

Zhelin Jin received his B.S. degree from Jiangsu University in 2021 and is now pursuing doctor's degree at Jiangsu University under supervision of Professor Guanggui Cheng. His research interests focus on triboelectric nanogenerator, self-powered sensors and intelligent electronic devices.

Ruifei Luan received her B.S. degree from Nanjing University of Posts and Telecommunications in 2021. She is now pursuing master's degree at University of Chinese

Academy of Sciences (Beijing Institute of Nanoenergy and Nanosystems, Chinese Academy of Sciences) under supervision of Professor Chi Zhang. Her research interests focus on tribovoltaic effects and tribovoltaic nanogenerator.

Likun Gong received his B.S. degree from China University of Petroleum (East China) in 2021 and is now pursuing doctor's degree at Jiangsu University under supervision of Professor Chi Zhang. His research interests focus on tribovoltaic effects and tribovoltaic devices.

Dr. Guoxu Liu received his Ph.D. degree from University of Chinese Academy of Sciences (National Center for Nanoscience) in 2021. He now is the assistant professor in Beijing Institute of Nanoenergy and Nanosystems, Chinese Academy of Sciences. His research interests are triboelectric nanogenerator, tribovoltaic devices and applications in energy harvesting and sensing.

Zhichao Jiang received the M.S. degree from Yanshan University. Now he is a doctor student at Guangxi University. His research interests include triboelectric nanogenerator, vibration energy harvesting and self-powered vibration sensing.

Jianhua Zeng received his Ph.D. from Guangxi University in 2024. He now is a lecturer at Guilin University of Electronic Technology. His research interests focus on triboelectric transistor and electronic skin.

Guizhang Ju received his BE degree from Xuzhou University of Technology and is now pursuing master's degree at Jiangsu University under supervision of Professor Guanggui Cheng. His research interests focus on triboelectric nanogenerator and self-powered sensors.

Letian Mi received his BE degree from Shandong University of Technology and is now pursuing master's degree at Jiangsu University under supervision of Professor Guanggui Cheng. His research interests focus on triboelectric nanogenerator and multimodal sensor.

Prof. Guanggui Cheng received his Ph.D. degree from Jiangsu University in 2010. After graduation, he worked at Tulane University, America as a visiting scholar. Now he is professor in school of mechanical engineering, Jiangsu University. Cultivated by the second level of "333" talents in Jiangsu Province. Prof. Guanggui Cheng's research interests are surface/interface science and technology, intelligent flexible mechanical electronic devices and systems, triboelectric nanogenerator and self-powered sensors/systems, and soft robot and actuators design.

Prof. Chi Zhang received his Ph.D. degree from Tsinghua University in 2009. After graduation, he worked at Tsinghua University as a postdoc research fellow and NSK Ltd., Japan as a visiting scholar. He now is the principal investigator of Tribotronics Group in Beijing Institute of Nanoenergy and Nanosystems, Chinese Academy of Sciences (CAS), Member of Youth Innovation Promotion Association, CAS. Prof. Chi Zhang's research interests are triboelectric nanogenerator, tribotronics, self-powered MEMS/NEMS, and applications in flexible

electronics, intelligent equipment and the Internet of things. He has been awarded by National Natural Science Foundation of China for Excellent Young Scientist Award.

Prof. Jianning Ding received his Ph.D. degree from Tsinghua University in 2001. Now, he is doing research in Yangzhou University as a professor. Prof. Jianning Ding's research interests focus on flexible mechatronics, new energy technology and equipment functional devices, including solar cell, flexible sensors, soft robotics, and so on.